THE STRENGTH AND FLEXIBILITY OF CORRUGATED AND CREASED-BEND PIPING.

A Dissertation Submitted to the
Advisory Board
of the
School of Engineering of the Johns Hopkins University
in conformity with the requirements for
the degree of
Doctor of Engineering.

By
ROBERT L. DENNISON
1935

REPRINTED FROM
JOURNAL OF THE AMERICAN SOCIETY OF NAVAL ENGINEERS,
VOLUME XLVII, NO. 3, AUGUST, 1935.
PAGES 343 TO 432.

THE STRENGTH AND FLEXIBILITY OF CORRUGATED AND CREASED-BEND PIPING.

A Dissertation Submitted to the
Advisory Board
of the
School of Engineering of the Johns Hopkins University
in conformity with the requirements for
the degree of
Doctor of Engineering.

By
ROBERT L. DENNISON
1935

REPRINTED FROM
JOURNAL OF THE AMERICAN SOCIETY OF NAVAL ENGINEERS,
VOLUME XLVII, NO. 3, AUGUST, 1935.
PAGES 343 TO 432.

R. UNIV.
BIBLIOTHEEK
LEIDEN

Copyright, 1935, by the American Society of Naval Engineers.

THE STRENGTH AND FLEXIBILITY OF CORRUGATED AND CREASED-BEND PIPING.

By Lieut. Robert L. Dennison*, U. S. Navy, Member.

I. INTRODUCTION.

1. *The General Problem of Design Involving High Temperatures and Pressures.*—The present day trend in the direction of higher steam temperatures and pressures as a means of increasing thermal efficiencies of steam cycles has necessitated the solution of many complex problems of engineering design. It may be said that the greatest barriers to the immediate utilization of the steam pressures and temperatures which theory indicates as being so desirable, are the lack of suitable metals and the lack of full knowledge of the behavior of available materials under conditions of temperature, stress, erosion, and corrosion. However, in many cases when the limitations of material are sufficiently known, the design is uncertain because of failure to foresee accurately under what conditions the material is to function in service. If the forces acting and the manner in which the act were known, if the stresses and strains which these forces produce in the material could be determined, and if the physical limitations of the material under the environmental conditions were fully appreciated, the optimum design could readily be accomplished. Ignorance of one or several of these design factors leads to the use of a so-called factor of safety. The machine element is designed so that the highest predicted stress multiplied by the factor of safety shall not exceed the yield strength or the ultimate strength, whichever is used as the basis for design. In some cases the fatigue limit is substituted for the yield strength or ultimate strength as the basis for the factor of safety, and at least one system of determining the allowable working stress is based on a combination of yield strength and fatigue

* Formerly attached to the U. S. Naval Engineering Experiment Station, Annapolis, Maryland.

strength*. The demands of low cost, minimum weight, and least space provide an ever increasing temptation to reduce the factor of safety. In order to do this intelligently, it is vitally necessary to possess full knowledge of all factors entering into the design and of those conditions in service which affect the strength of the material.

2. *The Design of Piping Systems.*—A typical problem exists in the design of steam piping. Increasing temperatures means that additional expansion must be absorbed. With high steam temperatures and long runs of piping, the expansion to be absorbed may be considerable. Four means for caring for pipe line expansion are generally accepted; swivel joints, expansion joints, slip joints, and the configuration of the piping system itself. Swivel joints are unsuitable except for low pressures and temperatures and are only used with small pipe sizes. The expansion joint is capable of absorbing little movement and is generally used under conditions where some materials such as rubber or copper might be successfully employed. Slip joints involve the use of packing and stuffing boxes. Because of leakage and uncertainty of action, they are seldom used at temperatures exceeding 400 degrees F. For high steam temperatures and pressures it is necessary to design a piping system so that the expansion may be absorbed by the deformation of the pipe line itself. This is usually accomplished by the inclusion of expansion bends or by changes in direction in the run of piping. It will be appreciated that where the expansion is taken up by the piping system, reactive forces will be exerted on the anchorages equal to those required to cause the necessary deflections in the piping. High reactive forces on the turbine flanges or boiler drums may cause serious distortion of these units. It is therefore desirable to have a high degree of flexibility in the piping system and hence small forces resulting from expansion.

3. *The Need for Flexible Piping.*—Because of the high reactive forces associated with the usual expansion elements, it became necessary to employ several such elements in runs of piping of moderate length. Where the steam piping changed direction large arcs were necessary because the usual piping requires the maintenance of a relatively large ratio of radius of curvature of the bend to the

* "Strength of Materials," Vol. 11, S. Timoshenko.

pipe diameter so as properly to form the bend. In order to provide increased flexibility and to permit forming of bends on a small proportion of the arc radius to pipe diameter, the so-called corrugated piping and creased-bend piping were developed. Typical examples of these pipe forms are shown on Plates IX and XI. These forms are in commercial use here and abroad.

4. *Objects of This Investigation.*—This investigation had the following objects: First, to determine the relationship between the load and deflection for various shapes of corrugated and creased-bend pipes in order to establish their flexibility relative to smooth-walled pipe; second, to determine the endurance properties of the corrugated and creased-bend pipes under cyclic stressing; third, to develop methods for measuring the strains induced in these pipes under load and interpreting the significance of these strains; and finally, to derive values for safe working stresses for these pipes for the purpose of piping system design.

II. PREVIOUS WORK.

5. *Early Experimental Work on Expansion Bends.*—In order to trace the development of the analysis of the strength and flexibility of pipe bends, it is desirable to review briefly the work of other investigators, not only on the creased and corrugated bends, but on smooth pipe bends as well. Perhaps the earliest important work was done by Dr. A. Bantlin of Stuttgart, who experimented with the lyre-shaped expansion bend,* sometimes called the double offset expansion U-bend. These experiments on smooth pipe showed that in the case of expansion bends formed of mild steel pipe the displacement of the ends when subject to forces tending to alter the curvature might be as much as five times greater than could be predicted by the ordinary theory of bending of curved bars. Dr. Bantlin concluded that the discrepancy between theory and measurement could be ascribed to a virtual reduction in the flexural modulus of rigidity, EI. This virtual reduction was believed to be caused by a large number of minute waves or folds on the inner side of the pipe bend which were formed in the bending of the pipe. Later, of course, the creased-bend pipes and corrugated pipes were designed

* "Formänderung und Beanspruchung federnder Ausgleichröhren," by A. Bantlin Zeitschrift des Vereines deutscher Ingenieure, January 8, 1910, p. 43.

in which folds were deliberately produced in order to augment flexibility.

6. *Development of the Theory of Flexibility of Pipe Bends.*—Dr. Th. V. Karman of Göttingen later analyzed the results of Dr. Bantlin's experiments and advanced the hypothesis that the discrepancies noted between measurement and theory were due to the deformation of the circular pipe section when the curvature of the bend was changed.*

It will be appreciated that when a pipe bend is subjected to couples acting on the ends tending to increase the curvature, the tensile forces in the pipe wall on the outside of the arc and the compressive forces in the pipe wall on the inside of the arc, lying in the plane of the bend, will each have components tending to force the walls in towards the neutral axis of the pipe. These components will tend to form the cross-section into a quasi-elliptical shape. This deformation will lessen the value of the moment of inertia of the cross-section of the pipe and will hence operate to increase the flexibility. The greatest cause of increased flexibility is, however, the relieving of stresses in the fibers farthest from the neutral axis of the pipe as a result of the flattening, with a consequent increase of the angular deflection of the bend before equilibrium of the internal resisting moment and external bending moment will occur. The effect on flexibility is equivalent to an increase in value of the bending moment or a decrease in the value of the moment of inertia of the cross-section of the pipe.

Hence, in finding the deflection of a curved pipe the value of flexural rigidity, EI, must become EI/K, where K is a dimensionless factor greater than unity.† K is expressed as a function of λ, where

$$\lambda = \frac{tR}{r^2} \text{ and}$$

* "Ueber die Formänderung dünnwandiger Rohre, insbesondere federnder Ausgleichröhre," by Th. V. Karman, Zeitschrift des Vereines deutscher Ingenieure, 11 November 1911, p. 1889.

† This factor, K, is defined by some authors as a factor less than unity and by others as the reciprocal of this value. As originally derived by Dr. Karman the factor had a value less than unity. The writer prefers to refer to this factor as having a value greater than unity. This convention will be followed in this paper in all cases where K appears.

t = thickness of pipe wall
R = mean radius of pipe bend
r = mean radius of cross-section of pipe
then

$$K = \frac{10 + 12\lambda^2}{1 + 12\lambda^2}$$

This expression for K is closely approximate for values of λ greater than 0.3. Dr. Karman applied this theory to the results of Dr. Bantlin's experiments and obtained close agreement.

7. *Researches at Massachusetts Institute of Technology.*—This important work by Dr. Karman did not attract much attention until Professor W. Hovgaard of the Massachusetts Institute of Technology undertook extensive investigations of the flexibility and strength of pipe bends.* Using an entirely different method of analysis, Professor Hovgaard proved the correctness of Dr. Karman's derivation of the value of K and checked the theory with observations on several pipe bends. The relieving of stresses in the fibers most distant from the neutral axis of the pipe in the plane of bending causes the longitudinal stresses not to follow a linear law but provides maximum values of stress nearer to this axis. Formulas for determining the value of the longitudinal stress were developed by both Karman and Hovgaard and were confirmed experimentally by the latter. It was also shown both experimentally and theoretically by Hovgaard that the transverse, or hoop, stresses which occurred at the ends of the major and minor axes of the deformed cross-section might, under certain circumstances be much greater than the longitudinal stresses.

8. *The Strength of Pipe Bends.*—The tests at the Massachusetts Institute of Technology were made with the pipes under static loading conditions only. A pipe bend was considered to have failed when its elastic range was exceeded. Hence, the object of the test was to discover the state of stress at which the pipe bend

* "The Elastic Deformation of Pipe Bends," by W. Hovgaard, Journal of Math. & Phys., Mass. Inst. of Tech., Vol. VI, No. 2, 1926.

"Deformation of Plain Pipes" and "Further Research on Pipe Bends," by W. Hovgaard, Journal of Math. & Phys., Mass. Inst. of Tech., Vol. VII, No. 3, October, 1928, and No. 4, December, 1928.

"Tests of High Pressure Pipe Bends," by W. Hovgaard, Journal of Math. & Phys., Mass. Inst. of Tech., Vol. VIII, No. 4, 1929.

would suffer a permanent set. This point was then taken as determining the limit of strength of the bend. The point of limiting strength, therefore, was taken at the limit of plasticity. It is important to appreciate this basis of estimating strength. Professor Hovgaard investigated the maximum strain energy theory according to Dr. M. T. Huber and Dr. H. Hencky, as defining the criterion of failure.* According to this theory the limit of beginning of plastic flow depends on the elastic work of deformation. When this work reaches a certain constant value at a given point, flow begins. The work of pure elastic deformation is given by the formula—

$$W = \frac{m + 1}{3\,m\,E}\,(p_1^2 + p_2^2 + p_3^2 - p_1p_2 - p_2p_3 - p_1p_3)$$

where p_1, p_2, p_3 are the principal stresses and m is the reciprocal of Poisson's ratio.

If W is constant its value at the yield point in one-axial tension may be expressed

$$W = \frac{m + 1}{3\,m\,E}\,p_0^2$$

where p_0 = the value of tensile stress at the yield point. Hence, in bi-axial stress

$$p_1^2 - p_1p_2 + p_2^2 = p_0^2$$

Hovgaard now assumes

$$p_e = (p_1^2 - p_1p_2 + p_2^2)^{\frac{1}{2}}$$

in which p_e is called equivalent stress.

Hovgaard found by analysis that, long before an appreciable permanent set occurred in the bends, this equivalent stress exceeded the yield point in certain sections of the pipe. These areas of high stress and plastic flow were considered to be localized and hence of not appreciable effect on the elasticity of the pipe as a whole. The longitudinal stresses in the outer surface of the pipe bend

* "Die spezifische Formänderungsarbeit als Mass der Anstrengung eines Materials," by M. T. Huber, Lemberg, 1904.

"Zur Theorie plastischer Deformation," Zeitschrift f. angew. Math. and Mech. Bd. 4, Heft 4, 1924, by H. Hencky.

appeared to reach the elastic limit at about the same time the permanent set began to appear. It was then assumed that the longitudinal stress determined the point of breakdown of pipe bends, and a formula is given for the determination of the maximum value of this stress. As long as this stress did not exceed about 20,000 pounds per square inch in the bends tested there was no permanent set. It was assumed that the yield point was about 25,000 pounds per square inch. Hovgaard made no distinction between "yield point" and "proportional elastic limit." The equation for the maximum longitudinal stress may be expressed

$$p_{max} = \beta \frac{Mc}{I}$$

$$\text{where } \beta = 2/3 \; K \left(\frac{6\lambda^2 + 5}{18}\right)^{\frac{1}{2}}$$

A curve is presented by Hovgaard for determining values of β for various values of λ. In closing the investigation, he recommended that, because of overstrains which will exist in certain parts of the pipe which might in time produce a permanent set, the designed working stress be taken as 16,000 pounds per square inch.

9. *Work of Other Investigators.*—Mr. A. M. Wahl carried out some investigations tending to confirm the work of Dr. von Karman and Professor Hovgaard.* Mr. Wahl considered the longitudinal and transverse stresses induced by bending of the pipe to be principal stresses, and proposed that the maximum shear theory be used as a means for determining the critical stress.† By this theory the strength depends on the maximum shear stress which is one-half the difference between the greatest and least principal stresses. The tensile stress equivalent to this shear stress will be equal to the difference between these principal stresses. Mr. Wahl developed a means for expressing this equivalent stress as a function of the longitudinal stress. He provided curves using Karman's factor as an argument to assist in the computation. Wahl also concluded that the internal pressure has no appreciable effect

* "Stresses and Reactions in Expansion Pipe Bends," by A. M. Wahl, Trans. Amer. Soc. Mech. Eng. FSP-50-49, 1927.

† J. J. Guest, Phil. Mag., Vol. 50, 1900, p. 69.

on the tendency of the cross-section of the bends to become elliptical under a bending moment. Mr. J. R. Finniecome, an English engineer, made a critical survey of the work on stress and deflections of pipe bends and concludes with Mr. Wahl that the maximum shear theory should apply.*

10. *Fatigue Failures of Piping in Service.*—In 1914 Mr. C. E. Stromeyer read a paper before the Institute of Naval Architects commenting on the cause of failure in the cases of about one hundred steam pipe ruptures in service.† The pipes which failed were of copper and were of various shapes. The failures occurred after the pipes had been in service from 24 hours to 10 years. Mr. Stromeyer, in this early work, attempts to estimate the fatigue stresses to which the individual pipes were subjected. At this time little was known about endurance properties of metals and the methods of calculating stresses in pipe bends. This work, however, indicates an important point which appears to have been overlooked in later work on determining limiting design stresses for pipe bends, namely, that service failures are associated with cyclic, rather than with static, stress application.

11. *The Flexibility of Corrugated and Creased Pipe Bends.*—Messrs. E. T. Cope and E. A. Wert have conducted numerous tests on various shapes and sizes of corrugated and creased pipe bends. These tests were for the purpose of determining the flexibility characteristics and were conducted with various types of loading.‡ They concluded that the flexibility of the corrugated pipe bend is due mainly to a change in tangential length, increasing on the outside of the bend and decreasing on the inside of the bend, while little flattening of the cross-section occurs. The creased bend appears to show somewhat less flattening of the cross-section than a smooth bend and owes its flexibility both to flattening and to the change in tangential length between creases. They determined the relationship between the measured flexibility of the corrugated and creased pipe bends and the calculated flexibility of smooth

* "The Flexibility of Plain Pipe," by J. R. Finniecome, The Engineer (England), August 17, 1928, p. 162; August 24, 1928, p. 199; August 31, 1928, p. 218; September 7, 1928, p. 246.

† "The Elasticity and Endurance of Pipe Lines," by C. E. Stromeyer, Engineering (England), June 19, 1914, p. 856.

‡ "Load Deflection Relations for Large, Plain, Corrugated and Creased Pipe Bends," by E. T. Cope and E. A. Wert, Trans. A. S. M. E., 1931.

pipe bends of similar shape, dimension, and under similar loadings. Messrs. E. A. Wert, S. Smith and E. T. Cope have developed a series of graphs for the purpose of determining the correct proportions for ten of the most commonly used shapes of pipe under various operating conditions.*

III. THE DESIGN OF PIPING UNDER CONSIDERATIONS OF VARIABLE STRESS.

12. *Operating Conditions of Steam Pipes in Service.*—There are many ways by which a steam pipe may be stressed in service. In superheat systems the variation in steam temperature causes a corresponding variation in pipe line expansion with consequent variable stress. Changes in steam pressure will likewise create stress cycles. The piping system is subjected to a stress cycle each time it is placed in and out of operation. In addition to these, mechanical vibration of a piping system will induce cyclic stresses which, even though of small magnitude, superimposed on an existing high state of steady stress may lead to failure. On shipboard the weaving of the ship's structure may induce serious variable stresses in the piping. Some or all of these conditions in varying degrees of severity will exist in any piping system.

A system of steam piping may be considered as a structure to absorb a certain strain induced principally by temperature change in the pipe. A structure subjected to a certain stress will, if this stress exceeds the yield strength of the metal, distort, buckle, and collapse. This series of events will in general characterize a static failure of ductile material. A piping system, however, is not subjected to this type of loading. Once the specified strain is absorbed, no further motion leading to collapse is possible. Repeated applications of strain, provided the resulting induced maximum stress is beyond the endurance limit for the metal, will lead to fatigue fracture.

It is difficult to visualize a service loading condition which would lead to piping failure with a single application of load. Professor Hovgaard in one of his papers shows a photograph of a 9½-inch pipe bend bent back upon itself so that the angle between the two

* "A Manual for the Design of Piping for Flexibility by the Use of Graphs," by E. A. Wert, S. Smith and E. T. Cope, published by The Detroit Edison Company in 1934.

parts was about 30 degrees.* There was complete collapse of the cross-section but no sign of fracture anywhere.

Under service conditions the ultimate failure of piping will be fracture resulting from repeated applications of stress caused by temperature changes, pressure changes, vibrations, or from relative movement of pipe anchorages. Elastic failure signalized by the passing of the yield point has no direct connection with the type of failure to be expected in piping systems. It is clear that variable stress, rather than static stress, considerations are the proper basis upon which to investigate the strength of pipe.

13. *The Mechanism of Fatigue Failure.*—If a reasonably ductile material, such as the steel from which steam pipes are commonly made, is subjected to steady load or only a few cycles of repeated load, highly localized stress will not cause appreciable damage provided the average stress is below the yield point of the material. In the areas where high local stresses exist, yielding occurs and the stress tends to equalize across the section. Where the material is under many cycles of repeated load of sufficient magnitude, the localized yielding leads to embrittling in these areas from cold work. The sliding of layers of metal within crystals, one upon the other, gradually leads to the development of minute cracks which spread and enlarge, leading to ultimate fracture. It will be appreciated that the area of highly localized stress may be small and that plastic flow may occur in this region long before the elastic properties of the piece as a whole may appear to be effected.

It appears that for all metals a limiting stress exists below which no fracture will occur even after the application of an indefinitely large number of cycles of stress. This limiting stress for most steels is established between 10^6 and 10^7 cycles of reversed stress. As the stress is raised above this limit the failure will occur at fewer numbers of cycles. The limiting stress is known as the endurance limit of the metal. In all cases the endurance limit is well below the static tensile strength and has been determined usually to be a certain percentage of this latter value. There does not appear to be any connection between the endurance limit and the elastic limit as measured in static tests.

* "Further Research on Pipe Bends," p. 255, loc. cit.

Local areas of high stress may be caused by abrupt changes in sectional dimensions such as at a hole in a plate, or at a shoulder on a bar. Likewise scratches, grooves, notches, or internal discontinuities in a metal will cause localized concentration of stress. A serious condition arises when corrosion of metal is accompanied by cyclic stressing. The cyclic stress accelerates the corrosion and the corrosion in turn causes areas of high stress concentration in the corrosion pits and cracks. This mutually intensifying action will lead to early failure or failure at considerably lower stresses than indicated by values of the endurance limit.*

14. *The Limitations of the Theory of Elasticity in Analyzing Stress in Corrugated and Creased Bend Piping.*—The mathematical theory of elasticity based on the work of Saint Venant affords a means of determining the distribution of stresses in many complex shapes. Often, however, the application leads to differential equations which are impossible of solution. The fundamental assumptions underlying the theory are that the material in which the state of stress is to be investigated is perfectly elastic, that it is homogeneous, that it is infinitely divisible, and that it is isotropic. Although obviously these assumptions are not valid in the case of most materials, such as steel for instance, the method yields results which represent an average correctness for the aggregate of crystals which go to make up the structure of the metal. In certain cases where two-dimensional problems of elasticity are to be solved, recourse may be had to photoelastic methods where exact mathematical solutions may not be obtained.

The analysis of the state of stress existing in the corrugated and creased bend piping under various types of loading appears to be a problem for which no rigorous mathematical solution is possible.

15. *The General Scheme of Investigation.*—The presence of corrugations or creases in a pipe, while increasing the flexibility, also acts to increase the stress. If fatigue tests are made on these pipes so as to determine an endurance limit for each given type, it will develop that the stress at this endurance limit when computed from the ordinary Rankine formulas of mechanics is far different from

* For an excellent summary of this complex subject see "Corrosion-Fatigue of Metals," by H. J. Gough, the Journal of the Institute of Metals (England), Vol. XLIX, 1932. Also "The Influence of Chemically and Mechanically Formed Notches on Fatigue of Metals," by D. J. McAdam, Jr., and R. W. Clyne, Journal of the National Bureau of Standards, Vol. 13, October, 1934. This paper includes a selected bibliography.

the stress corresponding to the known endurance limit of the steel. For the purpose of determining the stress at which the pipes were operated in fatigue tests the bending formula was used

$$S = \frac{Mc}{I}$$

In this formula, M is the value of the applied bending moment, I/c is the value of the section modulus of the basic pipe. In order to determine this value, the moment of inertia, I, of the cross-section was computed from dimensions of the pipe before being corrugated or creased. The value of c was likewise taken as the radius of the outer surface of the basic smooth-walled pipe. This equation then yields values for stress, S, which are nominal values. The term "nominal stress" has been applied to this quantity. The ratio of the endurance limit for the steel to the endurance limit of the pipe, when the latter is expressed in terms of nominal stress, will then be a direct indication of the stress multiplication effect due to the corrugated and creased bend shapes. The writer has called this factor the "stress intensification factor" and has given it the designation N.

In addition to the determination of the stress intensification factor, a method was developed for determining the stress distribution in pipes from internal pressure and from applied bending moments. This method employs the use of strain gages applied to the outside of the pipe wall and involves the calculation of the critical stresses at the inner pipe wall surface derived from these external strain measurements.

IV. MATERIAL UNDER INVESTIGATION.

16. *Classification of the Various Types of Piping.*—This investigation covers three classes of pipe shapes, all constructed from 6-inch seamless steel tubing as follows:

Series A—Corrugated piping with nominal wall thickness 0.280 inches and shape of corrugation as shown on Fig. 1, Plate I.

Series B—Corrugated piping with nominal wall thickness 0.288 inches and shape of corrugation as shown on Fig. 2, Plate I.

Series C—Creased bend piping of a typical shape of crease as shown in Plate II and with nominal wall thickness 0.288 inches.

Complete tabulations of the pipe shapes investigated under each of the above classifications, together with details of heat-treatments and physical properties, are given in Plates III and IV.

17. *The Individuality of the Corrugation and Crease.*—In manufacturing a corrugated pipe the seamless steel tubing is placed in a press between a fixed and movable head. A gas-fired ring furnace is placed around the pipe and a narrow band heated. When the pipe has reached a proper temperature, it is compressed along its axis by the press, thus raising a corrugation in the heated section. When the compression has raised the corrugation a desired amount, the press is stopped, the corrugation quenched, and the furnace moved on to form the adjoining corrugation. The first motion of the press, in forming a corrugation, causes an upsetting of the metal in the heated band before the swelling starts. This action accounts for the increased wall thickness to be found in the radial section through the crest of the corrugation. If a bend is to be formed, the bending is done after the corrugating process. The fabrication is followed by a suitable annealing heat-treatment.

In forming a creased bend, the pipe is first filled with sand, locally heated at each crease in turn, and bent about 10 degrees at each crease. The creases thus bulge out from the original pipe wall and disappear at about two-thirds of the circumference of the pipe. This method of bending is said to have the advantage of permitting bending without a thinning of the wall on the outside of the bend and a thickening of the wall on the inside of the bend. Both corrugated and creased pipe may be made with much smaller radius bends than may be formed from corresponding smooth-walled tubing. The processes of manufacture are patented.

It is to be carefully noted that the method of manufacture results in each corrugation or crease being an individual with possibly different characteristics than its neighbors. Non-concentricity of the bore of the tubing with the outer surface may be serious if it provides a minimum section in the plane of maximum stress. Because of the localized stress conditions in these pipes, it is also highly important that no local defects such as inclusions, laps, seams, or surface cracks appear in the tubing, because of the danger that one of these areas of weakness occur in a location of maximum stress.

V. EXPERIMENTAL METHODS—THE DETERMINATION OF THE ENDURANCE LIMIT OF THE PIPING.

18. *The Types of Testing Machines Used.*—Two types of testing machines were used to determine the endurance properties of the pipes. One type of machine was designed to apply a specific stress to the specimen and the other type a specific strain.* The specific stress machine was, in principle, a large scale model of the rotating beam fatigue testing machine frequently used in the laboratory for determining the endurance limit of small specimens. The specific strain machines were designed to subject the pipe to alternating flexure by applying a constant deflection to the specimen. A total of four machines of both types was built.

A view of the specific stress rotating beam testing machine is given in Plate V. Naturally only the long tangent specimens could be adapted to this apparatus. As will be seen from the plate, the long tangents were mounted in trunnion bearings at either end. Babbitt metal journals cast on the pipe carried collars which supported the desired dead weight load. The pipes were rotated by a motor and belt drive through a universal joint. With equal loads applied to the arms hanging from each collar, the bending moment across the corrugated section of the tangent was very nearly uniform. Hence all corrugations between the journals were subjected to approximately equal stress, and failure could reasonably be expected to occur in the weakest corrugation. With the pipe section at rest under load, the stress distribution in the pipe wall may be considered to be symmetrical with respect to a horizontal plane through the longitudinal neutral axis of the pipe. Now if the pipe is rotated 180 degrees, the fibers which were in the top half-section under certain states of stress, will acquire an equal value of stress but with opposite sign. This same reasoning applies to the fibers originally in the bottom half-section. Thus for a complete revolution of the pipe each fiber passes through a complete stress cycle from a maximum positive value of stress through an equal minimum negative stress value back to the positive stress value. In this

* See "The Fatigue of Metals," by H. J. Gough (London), 1924. According to Gough's classification a specific stress testing machine is one which applies a definite load on the specimen for each cycle. The load remains constant throughout the test. A specific strain testing machine is one which produces a definite deformation of the specimen for each cycle. In this type the deformation remains constant throughout the test.

investigation the pipe rotative speeds ranged from 80 revolutions per minute to 220 revolutions per minute. The speeds were carefully selected so that the pipe rotated smoothly and without vibration.

Two kinds of specific strain machines were developed. Views of these machines may be seen in Plates VI and VII. Two machines of the first kind were built. These machines each consisted of a 25 horsepower motor driving, through suitable reduction gearing, a shaft at right angles to the armature shaft extended. This driven shaft carried at either end an adjustable eccentric upon which a journal was mounted. The eccentrics could be adjusted to give the desired crank throw for the journal. This journal was connected through a vertical connecting rod to a suitable point to apply load on the pipe section. The cycle frequency in these machines ranged from 30 to 90 cycles per minute.

The remaining specific strain type of machine was developed from the water end of a reciprocating pump. The pump was mounted with its rod horizontal and with a hydraulic system, under pressure, connected to either end of the pump cylinder. The water was alternately admitted to one end of the cylinder and discharged from the other through an arrangement of plug cocks whose action was governed by a linkage operated from an electric motor. With the apparatus in operation, the pump rod would move back and forth at a cycle frequency of approximately 20 per minute. The amount of rod movement could be adjusted by suitable setting of the linkage mechanism to the plug cocks and could be positively limited by adjustable stops attached to one of the pump tie rods. The outer end of the pump rod was attached to a pipe flange for endurance testing purposes. This machine was used for testing certain expansion U-bends only.

19. *The Correlation of Results Obtained from the Specific Stress and Specific Strain Fatigue Testing Machines.*—In the specific stress type of fatigue testing machine the bending moment could be determined from the applied loading. The machine was equipped with an electrical device arranged so that if the pipe under test should begin to rotate eccentrically or should fracture completely, the drive motor would stop. The time of actual failure, that is, when a fatigue crack developed completely through the pipe wall, was anticipated by a short period of slightly eccentric rotation of

the pipe before this eccentricity became severe enough to signalize complete failure.

In the specific strain fatigue test, the load-deflection characteristics of the pipes were first determined. The points of application of load and the direction in which the loads were applied corresponded to the conditions of loading of the specimens in the fatigue testing machine. With the load-deflection relationship established, the bending moment and hence the nominal stress, as defined above, could be determined for a given deflection setting of the machine. The usual procedure in testing was first to select a desired value for the maximum nominal stress to be imposed in the pipe specimen, then to determine from the beam formula the load to be applied, and finally to set the fatigue testing machine to provide the corresponding deflection as established from the load-deflection curve for that specimen. As with the rotating beam specimens, the point of failure was taken to be when a fracture had occurred completely through the pipe wall. In order to assist in the detection of such a crack, the pipes were coated with white wash before testing. No automatic means for stopping the machine at the time of failure could be devised. Hence close inspection of the pipes on the running tests was necessary.

It will be appreciated that, if yielding occurs as a fatigue crack develops, the actual load to maintain a constant deflection will be reduced in the specific strain type of machine. This reduction in applied load causes a proportional decrease in the applied stress which might tend to increase the time required for ultimate failure. Laboratory testing experience indicates, however, that fatigue cracks progress rapidly to failure when once started, and that close agreement in results may be expected in testing with specific stress and specific strain type machines.

20. *The Effect of Range of Stress on Fatigue Strength.*—When a material is subjected to cyclical variations of stress the range of stress is defined as the algebraic difference between the maximum and minimum stresses of the cycle. The range ratio is equal to the minimum stress divided by the maximum stress. Thus for the case of a completely reversed stress, or what is usually termed alternating stress, the range ratio is —1.0. A range ratio of 0 would indicate that the stress varied from 0 to a maximum. The range ratio can never have a value greater than 1.

Several investigators have developed formulas and diagrams in order to define the relationship between stress range and fatigue strength. Gerber's parabola, Goodman's dynamic law, the formulas of Launhardt and Weyrauch, and the formula developed by J. B. Johnson are perhaps the best known of the earlier work on the subject. Much of this work did not check particularly well with later experimental determinations. The Goodman diagram for instance, implies that the endurance limit of a metal under alternating stress is one-third of the static ultimate tensile strength. This has been proven to be incorrect for many metals, particularly in the ferrous group. This diagram, however, further implies that the ratio between the endurance limit for a stress range from 0 to a maximum and the endurance limit for a complete reversal of stress is 1.5 to 1. This value was investigated by Professors Moore and Kommers, who concluded that it was a reasonably safe assumption for all metals.* They proposed a formula having the general form of the Johnson formula but not based on any assumed ratio of endurance limit to ultimate static tensile strength and retaining the Goodman ratio of 1.5.

$$S_{max} = \frac{.3\ S_{-1}}{2 - r}$$

where r is the range ratio,

S_{max} is the maximum unit stress during a cycle, and

S_{-1} is the endurance limit for alternating stress.

In the writer's investigation only two stress cycles were used; one a complete reversal of stress, and the other with stress varying from 0 to a maximum. In order to reduce the results of these tests to an equivalent basis to enable plotting failures associated with each of the two stress cycles to the same scale and on the same fatigue graph, the values of stress at failure in the case of the stress cycle from 0 to a maximum were divided by 1.5. This follows from the formula of Moore and Kommers.

21. *The Relationship Between Cycle Frequency and Endurance Limit.*—The stress cycle frequency does not appear to have much, if any, effect on the fatigue resisting properties of metals. H. J. Gough summarizes the results of various investigators in this field,

* "The Fatigue of Metals," Chapter VII, by H. F. Moore and J. B. Kommers.

who all concluded that no speed effect exists.* The cycle frequencies investigated varied from 150 to 5000 cycles per minute. The number of cycles of stress applied to a metal is said to be the controlling factor and the frequency of stress application is not significant. The case is very different when corrosive conditions are present together with the application of stress. The stress and corrosion have a mutually intensifying effect, but, since corrosion may also proceed without simultaneously applied stressing, the total time of the action is of great importance. The effect of cycle frequency on corrosion-fatigue is complex and depends upon many variables. This problem has been thoroughly studied by Dr. D. J. McAdam, Jr., who investigated cases of variations of cyclic frequency of from 1 per day to 10,000 per minute.† It may be mentioned that the cases of the cycle frequency of 1 per day include a boiler explosion after approximately 13 years' service.

22. *The Endurance Limit for the Steel from Which the Piping Used in This Investigation Was Fabricated.*—It was not considered practicable to machine satisfactory fatigue test specimens from the sample pipes used in this investigation. It is not necessary, however, to determine the actual endurance limit of this steel by direct test. It is generally accepted that a metal's endurance limit under cycles of reversed flexural stress may be expressed as a definite percentage of its ultimate tensile strength. No such correlation has been discovered between the endurance limit and any other physical property of a metal. The ratio of the endurance limit to the ultimate tensile strength has been termed the endurance ratio by Dr. McAdam, and for most steels will have a value of ranging between 0.40 and 0.50. Plate VIII gives a fatigue graph for a carbon steel whose composition was similar to the steel used in the pipe. This steel had a tensile strength of 63,000 pounds per square inch and an endurance limit of 27,000 pounds per square inch. The value of endurance ratio is hence 0.43. This value of endurance ratio has been applied to the observed tensile strength of the pipe steel in order to determine the value of its endurance limit.

In connection with Plate VIII it may be stated that the three points of highest stress on the fatigue graph were determined at a

* See "The Fatigue of Metals," Chapter V, by H. J. Gough.

† "The Influence of Stress Range and Cycle Frequency on Corrosion," by D. J. McAdam, Jr., Proc. of A. S. T. M., 1930, Part II, Technical Papers.

specimen speed of 50 revolutions per minute, while the points for the remainder of the graph were determined at 1450 revolutions per minute. The point representing the highest stress on this graph was obtained with a computed bending stress on the specimen actually greater than the ultimate tensile strength.

VI. EXPERIMENTAL METHODS—THE DETERMINATION OF THE FLEXIBILITY OF THE PIPING.

23. *The Necessity for Establishing the Load-Deflection Characteristics.*—Since the specific strain type of fatigue testing machine imposes a definte deflection on the pipe, the bending moments and the consequent applied nominal stresses could be determined only from a knowledge of the relationship between the load and deflection of the specimen under consideration. In order to establish the load-deflection characteristics, each pipe shape was mounted with one end firmly secured to a heavy steel foundation plate and dead weight loads applied to the other end. Deflections were measured by means of micrometers with increments of applied load. Small balls, acting as gage points for the measurements, were attached to the pipe flanges and to battens which were fixed to the foundation. Plates IX, X, XI and XII give views of typical arrangements for the load-deflection determinations.

24. *The End Conditions.*—Consider a pipe bend with its end flanges firmly fixed and subjected to an increase of temperature. The expansion of the pipe line will cause the flanges to exert certain forces and moments on the anchorages which may be resolved into a force perpendicular to the flange, a force parallel to the flange in the plane of the bend, and a couple also in the plane of the bend. This is called a fixed end condition. If the two forces continue to act but the couple is removed, the flange is thus permitted to rotate, and the condition is known as free end.

The fixed end condition was simulated in load deflection testing as shown in Plate X. Here the restraining force parallel to the flange in the plane of the bend is clearly 0. It is known from mechanics that a force and a couple acting in the same plane may be replaced by a single force whose moment arm is equal to the value of the couple divided by this force. It will be seen from the photograph that this is accomplished by the method of loading shown.

Here, as the load is applied, the flange moves in parallel planes. This condition was checked on test by a spirit level mounted on the upper flange. The proper value for the moment arm was first computed. Any subsequent minor adjustment necessary was indicated by the level.

Plate XI shows the simulation of the free end condition. Here the restraining moment is absent and rotation of the flange is therefore permitted.

There is a slight discrepancy between the state of affairs governing a load-deflection or fatigue test and the conditions actually obtaining in service. In the test conditions the forces and couples are applied on the cold or unexpanded pipe and hence on a pipe shape slightly different, from a dimensional standpoint, from the same pipe under elevated temperatures in service. This difference, however, is so slight that it may be disregarded for all practical purposes. It may be remarked that pipes in service will probably operate at some condition intermediate between the free end and fixed end conditions, and that the nature of these end conditions will have a decided effect on the stresses produced in the pipe itself.

25. *Results of Load-Deflection Determinations.*—Plates XIII to XVII, inclusive, give graphs showing the load-deflection relationship for each of the pipe shapes in the A, B and C series of piping. At least one pipe shape of each type was tested for each of the A, B and C series of piping. The remaining bends were checked for agreement with the typical similar shape before fatigue testing. The graphs also indicate the methods of loading and the points of deflection measurement. The effect of cold work on raising of the primitive elastic limit may be noted on those graphs which show the load-deflection characteristics after repeated loading.

26. *The Flexibility Factor.*—The flexibility factor V is defined as the ratio between the deflection of a section of corrugated or creased piping under a certain load to the deflection of a section of smooth-walled piping of the same length loaded in the same manner and by the same amount, both pipes considered to be the same basic wall thickness and same basic internal diameter. In brief, it is the ratio of the flexibility of the corrugated or creased pipe to the flexibility of a similarly dimensioned smooth-walled pipe. As is the case with the factor K, developed by Dr. Karman, the flexibility

factor V may be considered as modifying the flexural rigidity of the pipe shape considered.

In determining the flexibility of the piping, the grapho-analytical method of calculating deflections, combined with the principle of super-position, is used.* This method has been developed by The Detroit-Edison Company, which has published formulas for the areas of the bending moment diagrams, together with formulas for rotations and deflections, for various combinations of loadings applied to straight tangents and also quarter bends.†

It is proposed in the subsequent sections to investigate the value of the flexibility factor V for the following pipe shapes:

(*a*) The straight tangent, Series A.
(*b*) The straight tangent, Series B.
(*c*) The corrugated arc, Series A.
(*d*) The creased arc, Series C.

The flexibility factors to be developed will apply directly to the corrugated or creased bend shapes considered, and are entirely unassociated with the effect of added tangent lengths of piping. Thus, in computing the flexibility of corrugated tangents, the factor given applies to the corrugated section only, the effect due to the smooth pipe tangent length at the ends being eliminated by computation. Similarly, the flexibility factors given for the corrugated and creased arcs apply directly to the arc itself, and do not include the effect of tangent lengths beyond the 90 degrees of arc.

27. *The Flexibility of Straight Tangents–Series A.*—The moment area diagram for piece AC is shown as Figure 1, Plate XVIII.

$$(1)\quad EI\delta = \frac{\psi\ 1}{2}\ \frac{(4450\ V + 608) \times 75.75}{2}\ \text{Case II.}‡$$

(2) $I = 28.14$ (on basic pipe dimensions of 6.625 inches O.D. and 0.280 inches wall thickness).

(3) $\delta = 1.33 \times 10^3$ inches per pound load (Figure 1, Plate XIII).

* See "Applied Elasticity," by S. Timoshenko and J. M. Lessells, Section 23.

†A typical calculation involving the use of these methods is given in Appendix I.

‡ The case numbers mentioned in the calculations of Sections 27 and 28, refer to formulas shown in Plates XXXIX and XL. The methods used are demonstrated in Appendix I.

(4) $E = 29.7 \times 10^6$ pounds per square inch (by test).

Substituting from equations (2), (3) and (4) in (1), and solving for V:

(5) $V = 6.46$.

A similar computation for piece AA gives a value of $V = 6.4$.

28. *The Flexibility of Corrugated Arcs–Series A.*—The moment-area diagram for piece AH is shown as Figure 2, Plate XVIII. It is assumed that, as demonstrated in the previous section, the flexibility factor of the tangent sections of this bend is 6.5.

$EI\delta_c = \Psi_b 1$	$= 372{,}000$ F	down Case I
$= \Psi_f . 0.7854$ R	$= 7275$ VF	down Case V
$= \Psi_m . 0.637$ R	$= 19{,}750$ VF	down Case VII
$EI\delta_d = \Psi_c 1$	$= 754{,}000$ F + 81,600 VF	down Case I
$= \Psi_f \frac{2}{3} 1$	$= 160{,}100$ F	down Case II
$= \Psi_m \frac{1}{2}$	$= 23{,}600$ F	down Case III

(1) $\varepsilon EI\delta = 1{,}309{,}700$ F + 108,625 VF

(2) $E = 29.7 \times 10^6$ (by test)

(3) $I = 28.14$ (from section 27)

(4) $\delta = 2.50 \times 10^{-3}$F (Figure 2, Plate XIII).

Substituting from (2), (3) and (4) in (1), and solving for V:

(5) $V = 7.2$

This factor is approximately the same as the value of the flexibility factor for the straight tangent. As might be expected it is some what higher, possibly because of the deformation of the corrugations where the pipe is formed into an arc.

Dr. Karman's K value for a smooth-walled pipe arc of similar major dimensions is as follows:

$$K = \frac{10 + 12\lambda^2}{1 + 12\lambda^2}$$

$$\text{where } \lambda = \frac{tR}{r^2} = 0.584 \text{ and } \lambda^2 = 0.341.$$

(6) hence $K = 2.76$.

This indicates that this theoretical smooth pipe arc would be 2.76 times as flexible as an arc where no flattening occurred. This value of K for the smooth arc is comparable to the value of V for the corrugated arc. Hence, V/K = relative flexibility = 2.61. Therefore the corrugated arc is 2.61 times as flexible as a theoretical smooth arc having the same major dimensions.

29. *The Flexibility of Straight Tangents–Series B.*—The flexibility of the corrugated tangents of Series B, computed in the same manner as for Series A, gives the following results:

Piece BA, V = 6.4
Piece BB, V = 6.6
Piece BC, V = 6.4.

30. *The Flexibility of the Creased Arc–Series C.*—The flexibility of the creased arc of Series C, computed in the same manner as the corrugated arc of Series A, gives the following results:

Piece CA, V = 5.1
Piece CB, V = 5.0
Piece CC, V = 5.0.

The corresponding value of K for a theoretical smooth pipe arc of the same major dimensions is 3.79. Hence, assuming an average value of V to be 5.0, the creased arc appears to be approximately 32 per cent more flexible than the theoretical smooth arc.

31. *A Summation of Flexibility Results.*—The flexibility factor for all tangents tested may be taken as 6. Although the corrugated arc may show a slightly higher flexibility factor, this value of 6 should also be used for the arc in conservative design. Because of the increased flexibility of a smooth arc due to flattening, the corrugated arc shows an advantage in flexibility over the smooth arc of 2.6 to 1. Likewise the creased arc has a flexibility advantage of about 1.3 to 1.

VII. THE RESULTS OF THE FATIGUE TESTS.

32. *The Method Used in Developing the Graphs of Endurance Properties.*—The results of the fatigue tests of each of the series of corrugated and creased piping are shown graphically in Plates XIX, XX and XXI. The scheme used in plotting the fatigue graphs is the usual one for presenting results of fatigue testing. The axis

of ordinates is scaled uniformly to represent the semi-range of alternating stress while the axis of abscissas is scaled logarithmically to represent the number of cycles. The points on the graph, in general, indicate failures of the designated pipe shapes. In some cases the applied nominal stress values were raised during the test. Where this was done paths are shown on the graph to show the manner in which the specimen was tested at increasing stress values. Where arrows alone are attached to points this does not represent failure but means that the specimen is to be considered as continuing to run beyond the plotted point. The bending moments and the nominal stress were computed at the point of actual fracture for each specimen. The method of calculation employed was similar to that shown in Appendix I for the single offset quarter-bend, piece AM. In cases where the stress cycle varied from 0 to a maximum, the range was transformed for plotting purposes, as previously explained, to an equivalent range for alternating stress. The plotting of the fatigue graphs follows the practice in use at the U. S. Naval Engineering Experiment Station. Weight was given to the individual points, giving due regard to the effects of understressing and over-stressing on those specimens whose applied stress was raised in the progress of the test.

In all cases the nominal stresses, as previously defined, were computed from the simple beam formula as the stresses which would be produced in a theoretical smooth-walled pipe of the same basic dimensions as the corrugated or creased pipe when subjected to the same applied forces. The longitudinal stresses only were computed and in the comparative theoretical smooth-walled bend no allowance was made for any increase of stress caused by flattening. The direct stresses resulting from the loading are a small percentage of the stress due to bending and have, therefore, been neglected as minor in computing the nominal stresses.

33. *The Testing of Individual Specimens.*—In order to show clearly the circumstances attending the failure of each specimen, the details of the testing will be stated, treating the specimens individually.

SERIES A—PLATE XIX.

As a basis for determining the nominal stress the comparative theoretical smooth-walled pipe was assumed to have an outside

diameter of 6.625 inches and a wall thickness of 0.280 inch, thus having a section modulus of 8.5. The nominal stress was taken to be equal to the applied bending moment at the plane of fracture divided by the section modulus.

Straight Tangents.

The straight tangents were all tested in the specific strain type machine. The loading was applied in the same manner as shown for the load-deflection determination in Figure 1 of Plate XIII. The connecting rod of the machine was applied to the end of an I-beam which was secured at right angles to the pipe axis at the upper flange.

Piece AA was tested at a deflection setting to give a nominal stress range of 10,540 pounds per square inch varying from 0 to a maximum. Failure occurred after 121,840 cycles in the crest of the second corrugation from the base of the pipe.

Piece AB was tested at a deflection setting to give a nominal stress range of 12,920 pounds per square inch varying from 0 to a maximum. Failure occurred after 38,100 cycles in the crest of the second corrugation from the base of the pipe.

Piece AC was tested at a deflection setting to give an alternating nominal stress of 6900 pounds per square inch. Failure occurred after 198,164 cycles in the crest of the sixth corrugation from the base of the pipe.*

Expansion U-Bends.

Piece AD was erected for test as shown in Plate XXII. This was a fixed end test and, in addition, the pipe was placed under 400 pounds per square inch hydrostatic pressure. In order to eliminate corrosion as a factor, a 2 per cent solution of potassium dichromate was used as the liquid. This solution has strong properties as a corrosion inhibitor. The pipe was first put under internal pressure and then deflected so as to give a nominal stress range of 10,100 pounds per square inch varying from 0 to a maximum. The load-deflection relationship for this pipe was found to be the same

* Both the corrugation and the crease protrude beyond the original pipe wall. The crest of a corrugation or crease is considered as the region of maximum pipe diameter. The trough of a corrugation or crease is considered as lying between two adjacent crests and is therefore in the region of basic pipe diameter. These definitions are to be considered as applying where the terms "crest" and "trough" are used in this paper.

with the internal pressure of 400 pounds per square inch as without this pressure. Failure occurred at the point of maximum bending moment on the crest of the first corrugation from one end. Although the stress due to the applied bending moment varied from 0 to a maximum, the internal pipe pressure produced a state of steady stress in the pipe which caused the total stress to vary from a stress value different from 0. For this reason, the failure of this particular specimen should not properly be plotted on the graph of Plate XIX. It has, however, been placed on the graph for comparison purposes but has been disregarded in determining the fatigue curve. For purposes of plotting, it was assumed that the stress range ratio was 0.

Piece AE was tested in the pump gear specific strain type machine in the free end condition. A deflection was selected to give a nominal stress of 7040 pounds per square inch varying from 0 to a maximum. Failure occurred in a crest of a corrugation at the point of maximum bending moment after 316,900 cycles.

Piece AF was tested in the pump gear machine with one end fixed and the other end guided. An alternating nominal stress of 6280 pounds per square inch was imposed on the pipe. Failure occurred after 75,200 cycles in a corrugation trough near the point of maximum moment. This point of failure was on the inner arc of the pipe bend and because of the high arc curvature the corrugations were crimped closely together. This was the only failure observed in a corrugated pipe which did not occur in the crest of a corrugation.

Quarter Bends.

Piece AG was tested in the specific strain type machine with an alternating nominal stress of 5160 pounds per square inch. Failure occurred in the crest of the twelfth corrugation from the base after 288,700 cycles.

Piece AH was tested in a similar manner and failed in the crest of the sixteenth corrugation from the base after 267,400 cycles with an alternating nominal stress of 4140 pounds per square inch.

Straight Tangent Rotating Beam Specimens.

Piece AJ failed in the first and second corrugation crests from one journal after 1,178,780 cycles at an alternating nominal stress of 3660 pounds per square inch.

Piece AK failed in the crest of the sixth corrugation from one journal after 136,020 cycles at an alternating nominal stress of 6000 pounds per square inch.

Piece AL failed after 1,475,370 cycles in the crest of the fifth corrugation from one journal with an alternating nominal stress of 3060 pounds per square inch.

Single Offset Quarter Bend.

Piece AM was tested in the specific strain type machine as shown in Plate XXIII. This was a special type of bend curved to a sharp radius so that the corrugations were considerably flattened along the outer axis of the bend. This piece was tested with a nominal stress of 8400 pounds per square inch at the point of failure, varying from 0 to a maximum. The failure occurred after 78,105 cycles at a point where the actual computed nominal stress was approximately 16 per cent less than exerted at the point of maximum computed stress. This specimen should not properly be plotted in Plate XIX but has been placed there for comparison purposes and was disregarded in determining the fatigue graph.

SERIES B—PLATE XX.

As a basis for determining the nominal stress the comparative theoretical smooth-walled pipe was assumed to have an outside diameter of 6.625 inches and a wall thickness of 0.288 inch, thus having a section modulus of 8.7. The nominal stress values, computed for the point of actual fracture, were derived as previously explained.

Straight Tangents.

All straight tangents were tested in the specific strain type machine in a manner similar to that described for the straight tangents of Series A.

Piece BA was tested with a nominal stress cycle of 10,500 pounds per square inch varying from 0 to a maximum and failed in the crest of the seventh corrugation from the top after 200,480 cycles.

Piece BB was tested with an alternating nominal stress of 7840 pounds per square inch and failed after 94,400 cycles in the seventh corrugation from the base of the pipe.

Piece BC was tested with an alternating nominal stress of 11,300 pounds per square inch and failed after 26,700 cycles in two places, at the crests of the fourth and sixteenth corrugations from the base, and on opposite sides of the pipe.

Quarter Bends.

Three quarter bends, pieces BD, BE and BF, were constructed with a creased arc and with one corrugated tangent leg. Thus for purposes of plotting on the fatigue graphs they were considered as belonging to both the B and the C series.

Piece BD was one of the first specimens to be tested. No information was available concerning the location of the fatigue curve in the stress-cycle plane. This specimen was therefore tested at increasing values of stress in order to determine as quickly as practicable some probable limits for the location of this curve. This specimen was tested first with an alternating nominal stress of 2880 pounds per square inch for 63,605 cycles. The stress was then raised to 6950 pounds per square inch for 100,058 additional cycles. In the next step the nominal stress was raised to 10,100 pounds per square inch and failure occurred after an additional 5630 cycles of alternating stress. The failure occurred in the trough of the lowest crease. The specimen is therefore plotted as continuing on the graph for the B series corrugated pipe, since no failure occurred in the corrugated leg, and as a failure on the graph for the C series creased pipe.

Piece BE was tested in the specific strain machine with an alternating stress of 2220 pounds per square inch. In addition to this loading, a steam pressure of 100 pounds per square inch was placed on the pipe. No failure occurred after 2,830,624 cycles. This specimen is therefore plotted as continuing on each of the B series and C series graphs. The steam pressure was disregarded in computing the range ratio and the nominal stress, and the point of discontinuing the test plotted on the fatigue graph for both the B and C series.

Following this test, the pipe was carefully inspected both externally and internally. No evidence of damage could be discovered. Since the test had been run with a value of stress somewhat lower than the endurance limit it was unlikely that any damage would

have occurred. This specimen was then erected for test as before but with 400 pounds per square inch internal hydrostatic pressure. A solution of potassium dichromate was used as a liquid. The deflection was adjusted to give an alternating nominal stress of 5740 pounds per square inch. A failure resulted in the trough of the lowest crease of the arc after 201,361 cycles. The crack was welded and the test continued. A failure resulted in the crest of the tenth corrugation from the base after an additional 11,200 cycles. These failures of piece BE with 400 pounds per square inch internal pressure have not been plotted on the fatigue graphs. It may be seen, however, by reference to the curves that these points of failure lie in close proximity to the curves.

Piece BF was subjected to a nominal stress range of 15,850 pounds per square inch varying from 0 to a maximum. It failed after 24,805 cycles in the fourth corrugation from the top. It was therefore plotted as a failure on the B series graph and as continuing on the C series graph.

Straight Tangent Rotating Beam Specimens.

Piece BG was tested in the rotating beam machine with an alternating nominal stress cycle of 4390 pounds per square inch and failed after 307,250 cycles in the crest of the third corrugation from one journal.

Piece BH was similarly tested and failed in the crest of the fifth corrugation from one journal after 328,200 cycles of 5040 pounds per square inch alternating nominal stress.

Piece BJ was similarly tested and ran for 6,205,860 cycles at an alternating nominal stress of 2240 pounds per square inch. The stress was raised to give a cycle of 3420 pounds per square inch and failure then occurred in the crest of the first corrugation from one journal after an additional 22,970 cycles.

SERIES C—PLATE XXI.

As a basis for computing the nominal stress the comparative theoretical smooth-walled pipe was assumed to have 6.625 inches outside diameter and a wall thickness of 0.288 inch. Nominal stresses at the point of actual failure were computed as explained previously.

Piece CA was among the first specimens tested. In order to determine probable limits for the fatigue curve in the stress-cycle plane this specimen was tested at increasing values of nominal stress. It was first tested at 2330 pounds per square inch alternating nominal stress for 15,600 cycles, then at 4630 pounds per square inch for an additional 35,600 cycles, then at 6820 pounds per square inch for an additional 100,000 cycles, and finally at 9270 pounds per square inch when failure occurred after an additional 43,200 cycles. Failure occurred in the trough of the lowest crease of the arc.

Piece CB was subjected to an alternating stress of 6900 pounds per square inch and failed, after 108,000 cycles, in the trough of the first crease from the vertical tangent.

Piece CC was subjected to an alternating nominal stress of 3260 pounds per square inch for 5,200,000 cycles. The stress was raised to 4110 pounds per square inch for an additional 2,100,000 cycles, and failure finally occurred after an additional run of 720,000 cycles at a nominal stress of 5120 pounds per square inch. Failure occurred in the trough of the second crease of the arc from the vertical tangent.

Expansion U-Bends.

Piece CD was tested similarly to piece AD but without hydrostatic pressure, as shown in Plate XXIV. A nominal stress of 11,650 pounds per square inch varying from 0 to a maximum was applied. It failed in numerous places after 260,000 cycles.

Piece CE was tested in the pump gear machine with one end fixed and the other end guided. An alternating nominal stress of 6720 pounds per square inch was applied and failure occurred in the trough of a crease approximately at the point of maximum moment after 260,000 cycles.

Piece CF was tested with fixed ends and with 400 pounds per square inch hydrostatic pressure. The testing arrangement was similar to that shown in Plate XXII for piece AD. The nominal stress due to the applied bending moment varied from 0 to 8380 pounds per square inch. This is equivalent for plotting purposes to an alternating stress of 5580 pounds per square inch. Because of the steady stress due to internal pressure the true stress varied above and below some value different from 0. The test of this specimen

was, therefore, not plotted in Plate XXI. The testing was discontinued after no failure had been observed following 1,040,000 cycles of applied stress. It may be seen, by referring this performance to the fatigue curve of Plate XXI, that the strength of this pipe was apparently not adversely affected by the internal hydrostatic pressure.

VIII. THE NATURE OF FATIGUE FAILURES.

34. *The Location of the Fatigue Cracks in Corrugated Piping.*—Plates XXV and XXVI show photographs of typical failures in corrugated piping. The failure shown in Plate XXV occurred with the rotating beam type testing machine, while the other shown on Plate XXVI occurred with the specific strain type machine. The appearance of the fractured surface which is so characteristic of fatigue fractures clearly indicates that the crack progressed from the inner surface to the outer surface of the pipe wall. This conclusion was checked in many cases by observing the progress of the cracks in axial planes across the plane of failure. Planes could be found where the crack could plainly be seen to have failed to work its way entirely through the pipe wall. A photomicrograph of a typical crack is shown in Plate XXVII. This specimen was removed from piece AM, the single offset quarter bend, from the corrugation just above the one where complete fracture occurred. The crack shown in this photomicrograph had started from the inside surface of the pipe wall but had not progressed entirely through the wall thickness.

With but one exception, all failures of the corrugated piping took place in the transverse plane through the crest of a corrugation. From a study of the probable distribution of stresses in the pipe wall it seems clear that this would be the location of highest stress, and that the critical zone would be at the crest of a corrugation on the inside of the pipe, which is, of course, normally the surface of sharpest curvature. The one exception concerned the failure of piece AF, which has already been noted. Here failure occurred in the trough between two corrugations and the crack appeared to originate from the outside surface of the pipe. In this case the corrugations had been strongly crimped together on the inner side of the arc of the bend and the longitudinal radius of curvature of the surface at the point of failure appeared to be at least equally as

small as the radius of curvature of the inner surface of the adjoining corrugations.

Because, in general, the fatigue cracks do not start from the outside, it may be expected that a failure of corrugated pipe in service will not be detected until the crack has progressed entirely through the metal. The first warning in such a case may be a steam leak or perhaps a complete rupture. Once started, the progress of a fatigue crack is very rapid and a complete traverse of the metal will occur relatively soon after the inception of the crack.

35. *The Location of Fatigue Cracks in Creased Piping.*—In all cases of failure in creased piping the crack appeared to start from the outer surface and proceed inward. Without exception the failure occurred in the trough between two creases. This is the reverse of the manner in which failures occurred in the corrugated piping where the crack advanced from the inner to the outer surface.

The case of specimen CD, an expansion U-bend, presented an interesting example of fatigue failure. As has been explained, this specimen was tested with fixed ends with a stress cycle varying from 0 to a maximum. Hence the creased arcs were all on the compressive sides of the bends. The ultimate failure occurred in a zone of maximum bending moment from a crack developing from the outer surface inward and located in a trough between two creases. Longitudinal strips were cut from the pipe in the plane of the pipe bend. One strip was taken from half of each creased arc. The half chosen was the one subjected to the maximum bending moment. All four strips thus chosen were theoretically equally stressed. Plate II shows a photograph of the four strips selected for examination. The inner pipe surface is on the right of each strip. A total of 16 creased crests and 12 troughs was provided in these strips. A microscopic examination showed that 7 troughs contained incipient cracks, while 6 crests also showed cracking. There was a total of 10 cracks in the crests and 12 cracks in the troughs.

The appearance of the large number of cracks in the specimen CD is probably due to the nature of the test. It is possible that under the compressive cycle the crack associated with ultimate failure would not progress from inception to fracture with sufficient rapidity to fail to provide time for additional cracks to develop.

The creased crests, however, were probably in a state of tensile stress which might aid the rapid propagation of a fatigue crack.

In the case of a creased bend it appears probable that the appearance of an external surface crack would precede failure. However, the progress of the crack is likely to be so rapid that routine inspections could hardly be depended upon to predict such failure.

IX. THE ANALYSIS OF STRAIN.

36. *The Purpose of the Analysis.*—The results to be sought in this analysis are the expressions defining the state of strain at the inner surface of the pipe, more particularly, at the point of fatigue failure. In order to obtain these expressions the state of strain at the outer surface is determined experimentally and with certain assumptions as to the distribution of strains through the wall section, the state of strain at the inner surface will be deduced. The method is here presented as applying to a corrugated pipe. As will be shown, the same method, with some simplification, may be applied to the determination of the strains in the critical zone of probable failure in a creased pipe. The ultimate object in determining the strains is to establish the state of stress. The method of interpreting the results of the strain analysis in terms of stress will be developed in later sections.*

37. *Fundamental Considerations.*—In the following analysis certain fundamental assumptions are made. It is assumed that the material is perfectly elastic, that transverse cross-sections in bending originally plane remain so, and that the principle of superposition holds. The term "strain" will refer to the value of this quantity per unit length. Where the integrated value of strain over a length is to be indicated, the term "total strain" will be used.

A corrugated pipe shape may be considered to be formed by the revolution of the curve of the neutral axis of the corrugated wave shape about a longitudinal axis. In the zone of greatest interest, namely, the crest of a corrugation, the radius of curvature of the surface thus formed is large with respect to the thickness of the pipe wall. The radius of curvature of the corrugation itself is, however, not large with respect to the wall thickness. These two

* The writer has benefited by being permitted to refer to Dr. W. M. Coates' unpublished monograph on stress distribution in shells.

radii are designated as R_2 and R_1, respectively, and are indicated in Figure 5 of Plate XXIX. This diagram shows a longitudinal section and a hoop section of a corrugation. The system of designating the axes is also shown in the diagram. Thus 1 refers to the longitudinal direction, 2 to the hoop direction, and 3 to the radial direction. These three axes are mutually perpendicular.

The fact that R_1 is small compared to the wall thickness causes a thin shell analysis of strain to be invalid and necessitates knowledge of the position of the longitudinal neutral surface with respect to the inner and outer surfaces, as well as knowledge of the manner of strain distribution through the section, in order to deduce the value of inner surface strain from outer surface measurements.

The strains across the shell thickness are considered as of two classes:

(*a*) Uniformly distributed or membrane strains,
(*b*) Non-uniformly distributed or bending strains.

These categories include strains in the shell caused directly from the shell loading or those induced in one direction by strain in a direction perpendicular to it. The bending strains are associated with a relative change in angular displacement of the normals to the neutral surface.

Compressive strains are to be considered as negative in sign and tensile strains as positive.

38. *The Strain Distribution.*—

Notation.

E_{1_e} = Resultant longitudinal strain at outer surface of shell.
E_{2_e} = Resultant hoop strain at outer surface of shell.
ε_{1_e} = Longitudinal bending strain at outer surface of shell.
ε_{2_e} = Hoop bending strain at outer surface of shell.
ε_{1_m} = Longitudinal membrane strain constant throughout the shell thickness.
ε_{2_m} = Hoop membrane strain constant throughout the shell thickness.

The subscript i, used in place of e, refers to the inner shell surface.

The linear strain measured at the shell surface will consist of two components, bending strain and membrane strain. If the bending strain may be determined from the measurement of angular normal displacements, and if the total strain may be determined from measurements of surface extension, the value of the membrane strain may be obtained by subtraction. These considerations lead to the equations for the resultant strains—

$$(1)\quad E_{1_e} = \varepsilon_{1_e} + \varepsilon_{1_m}$$
$$(2)\quad E_{2_e} = \varepsilon_{2_e} + \varepsilon_{2_m}$$

These equations define the longitudinal and the hoop strains at the outer surface of the shell. At the inner surface, the bending strains will have reversed sign and will, in general, differ in absolute value. The membrane strains at the inner surface will, by definition, be identical in size and value with the membrane strains at the outer surface. Assume that

$$\left|\frac{\varepsilon_{1i}}{\varepsilon_{1e}}\right| = k_1 \text{ and that } \left|\frac{\varepsilon_{2i}}{\varepsilon_{2e}}\right| = k_2$$

then—

$$(3)\quad E_{1_i} = E_{1_e} - \varepsilon_{1_e} - k_1\varepsilon_{1_e}$$
$$(4)\quad E_{2_i} = E_{2_e} - \varepsilon_{2_e} - k_2\varepsilon_{2_e}$$

These equations define the longitudinal and hoop strains at the inner surface of the shell.

In the hoop section, the radius of curvature of the neutral surface is large compared to the shell thickness. Hence the position of the neutral surface may be taken as identical with the mid-surface as with thin shells. The value of k_2 is therefore one, and the bending strain is distributed linearly across the thickness.

In the longitudinal section, the shell must be considered as thick and the value of k_1 must be mathematically or experimentally determined since the bending strain distribution across the section will not follow a linear law.

39. *The Bending Strain.*—

$$(5)\quad \varepsilon_z = \frac{z\,d\Theta}{(R + z)\,d\,\beta}$$ (By definition, from Figure 1, Plate XXIX)

where ε_z is the bending strain on the surface whose radius of curvature is $(R + z)$, or—

$$(6)\quad \varepsilon_z = z\frac{d\Theta}{ds'}$$

where $ds' = (R + z)\, d\beta$

40. *Methods of Strain Measurement—The Resultant Strains.*—The Huggenberger Tensometer was used for measuring directly the resultant strains. A view of this instrument may be seen in Plate XXX. The movement of the knife edges is magnified approximately 1200 times on the scale. The knife edges may be adjusted to various gage lengths. In this investigation gage lengths of one-quarter inch in the longitudinal direction, and one inch in the hoop direction, were used.

41. *Methods of Strain Measurement—The Bending Strains.*—A method of measuring bending strains has been described by Huggenberger.* Plate XXXI shows a bending strain gage constructed after his schematic diagrams. The bases of the instrument legs are fixed to small rods soldered to the surface to be measured. Figure 2 of Plate XXIX gives a diagrammatic sketch of the action of the instrument in measuring bending strain. The dotted lines in the diagram indicate the relative positions of the instrument parts after the surface to which it is attached has been placed in pure bending. The angular rotation of the legs of the instrument may be considered as taking place about the neutral axis MN. From the Figure, it will be seen that—

$$(7)\quad RS = (d + h)\, d\Theta$$

$$(8)\quad dL = RS\left(\frac{m + n}{m}\right) = (RS)g$$

where g is the magnification factor of the instrument.

$$(9)\quad d\Theta = \frac{dL}{g\,(d + h)}\ [\text{from (7) and (8)}]$$

then

$$(10)\quad \varepsilon_e = \frac{h}{g\, ds'\,(d + h)}dL\ [\text{from (9) in (6) assuming } z = h]$$

* "Ueber die Festigkeit der Gewölbten Böden und der Zylinderschale by Höhn, Berlin, 1927, Part II, by Huggenberger.

In pure extension the reading of the strain gage will be simply the relative movement of the rods at the surface multiplied by the multiplication factor, or

$$(11)\quad dL' = gds'\varepsilon_m$$

If the surface on which the strain gage is applied is subjected to a combination of bending and tensile strains, then the reading of the instrument will be the sum of the individual readings of each component considered separately, or

$$(12)\quad dL'' = dL + dL'$$

then

$$(13)\quad dL'' = gds'\varepsilon_m + gds'\left(\frac{d + h}{h}\right)\varepsilon_e$$

Generalizing equation (1)—

$$(14)\quad E_e = \varepsilon_e + \varepsilon_m$$

Solving equations (13) and (14) as a simultaneous system—

$$(15)\quad \varepsilon_e = \frac{h}{d\ (ds')}\left(\frac{dL''}{g} - ds'E_e\right)$$

This equation may be written as applying to the longitudinal and hoop directions as follows:

$$(16)\quad \varepsilon_{1_e} = \frac{h_1}{d\ (ds')}\left(\frac{dL''}{g} - ds'E_{1_e}\right)$$

$$(17)\quad \varepsilon_{2_e} = \frac{h_2}{d\ (ds')}\left(\frac{dL''}{g} - ds'E_{2_e}\right)$$

These two equations, in addition to equations (1), (2), (3), and (4), are sufficient to determine the state of strain at the inner surface from measurements made on the outer surface. E_{1_e} and E_{2_e} are determined directly from the tensometer readings, knowing the multiplication factor of this instrument and the gage length. The value for dL″ is taken directly from the reading of the bending strain gage. The application of these formulas, however, involves the value of h, which is the distance from the outer surface to the neutral axis and also involves values of k_1 and k_2, which are the

absolute values of the ratios of the bending strains at the inner surface to the bending strains at the outer surface in the longitudinal and hoop directions, respectively. As has been previously explained, the value for k_2 may be taken as 1.

The value for h_2 may likewise be taken as equal to one-half the wall thickness. The determination of the proper values for h_1 and k_1, however, requires further analysis. The solution for stress (and strain) distribution in curved bars in pure bending is applied to this analysis.

42. *The Determination of the Position of the Neutral Axis and Hence the Values of h_1 and k_1.*—The location of the planes of failure in the fatigue tests indicates that the section of principal interest lies at the intersection of a transverse plane passing through the crest of a corrugation, with the pipe wall. Because of the initial upsetting of the metal when the corrugation is formed, the outer and inner surfaces of the corrugation in a longitudinal plane will not have the same centers of curvature. For purposes of analysis the outer radius of curvature at the critical section is taken to be equal to the radius of curvature of the inner surface plus the wall thickness at this section. It is further assumed that the corrugation is symmetrical about an axis defined by the transverse plane for a sufficient arc length to encompass the region over which the strain measurements were made. With these approximations and assumptions the solution for stress distribution in pure bending of curved bars is used for the determination of the position of the neutral axis of a longitudinal section of the pipe wall.* The radius of curvature of the hoop section is considered to be large in proportion to the radius of curvature of the longitudinal section and hence to exert no sensible effect on the position of the neutral axis of this latter section.

The value of the tangential stress in a curved bar in pure bending is given by the equation:—

$$(18)\quad \sigma_\Theta = -\frac{4M}{N}\left(\frac{-a^2b^2}{r^2}\log b/a + b^2\log\frac{r}{b} + a^2\log a/r + b^2 - a^2\right)$$

where M = bending moment, and

$N = (b^2 - a^2)^2 - 4\,a^2b^2\,(\log b/a)^2$, and

a, b and r are the radii of curvature of the inner surface, outer surface and neutral surface, respectively.

* The solution here given is from "Theory of Elasticity," Chapter 3, by S. Timoshenko.

The right hand member of equation (18) was set equal to 0 and solved for r/a in terms of b/a. The result of this solution is shown in Plate XXXII. From this graph, knowing the values of b and a, the value of r and hence the location of the neutral axis may readily be determined.

Equation (18) was also solved for simultaneous maximum and minimum values for various values of b/a. The result of the computations are given graphically on Plate XXXIII where the values of k_1 may be read directly from the ordinate scale. These values for k_1 are practically the same as would be obtained by assuming a hyperbolic distribution of the bending strain across the shell thickness. In the determination of the values of k_1 and h_1 in the piping under test, the values for the dimensions of the radii of curvature of the inner and outer corrugation surfaces were taken as the average of a large number of measurements of corrugated sections. The average results of these measurements are shown in Figure 4 of Plate XXIX.

X. THE ANALYSIS OF STRESS.

Notation.

$\sigma_1, \sigma_2, \sigma_3$ = Normal components of stress parallel to 1, 2 and 3 axis.

ν = Poisson's ratio.

E = Modulus of elasticity.

$\varepsilon_1, \varepsilon_2, \varepsilon_3$ = Strains in 1, 2 and 3 directions.

σ_n = The value of stress at the endurance limit in reversed flexural stress.

σ_e = An equivalent tensile stress.

43. *The Determination of the Principal Stresses.*—It may be seen from considerations of symmetry that the principal axes at the inner surface of the crest of a corrugation are as indicated in Figure 5, Plate XXIX. The values of strain along axes 1 and 2 may be determined as explained in the previous section on strain analysis. It will now be shown, given these strain values in the longitudinal and hoop direction, how the values of the principal stresses may be determined.

It follows from Hooke's law that the three normal components of stress parallel to three mutually perpendicular axes may be expressed :—*

$$(19)\ \sigma_1 = \frac{\nu E}{(1+\nu)(1-2\nu)} e + \frac{E}{1+\nu} \varepsilon_1$$

$$(20)\ \sigma_2 = \frac{\nu E}{(1+\nu)(1-2\nu)} e + \frac{E}{1+\nu} \varepsilon_2$$

$$(21)\ \sigma_3 = \frac{\nu E}{(1+\nu)(1-2\nu)} e + \frac{E}{1+\nu} \varepsilon_3$$

where—

$$(22)\ e = \varepsilon_1 + \varepsilon_2 + \varepsilon_3$$

If the axes selected are the principal axes, the shearing components of stress vanish and equations (19), (20), and (21) completely define the state of stress on the sides of an element which are parallel to the coordinate planes.

The methods of strain analysis yield values for ε_1 and ε_2 (which are equivalent to E_{1_i} and E_{2_i} determined as described above), thus considering equations (19), (20), (21), and (22) there are four equations and five unknowns. This system of equations is then insufficient to provide a solution for the unknown quantities. In the cases of pipe loadings from bending moments alone, the value σ_3 is clearly 0. Also where the loading is from internal pressure, the value of σ_3 is equal to the value of this pressure. Hence in all cases the value of σ_3 may properly be assumed and the system of equations solved for σ_1 and σ_2.

With the assumption of the value for σ_3, the values of the principal stresses are now known.

44. *The Maximum-Shear Theory Applied to Fatigue Failures.*— The endurance limit of metals in shear, according to data assembled by Moore and Kommers, has a value of about 55 per cent of the endurance limit in reversed direct stress.† This fact indicates that the maximum-shear theory of the failure of metals is a safe approximation for cases where fracture occurs from fatigue.‡

* See "Theory of Elasticity"—Timoshenko—Introduction—or any text on elasticity.
† "Fatigue of Metals," by Moore and Kommers.
‡ See paper by J. J. Guest, loc. cit.

Since the maximum shearing stress is equal to half the difference between the maximum and minimum principal stresses, the condition for failure from fatigue is:

$$1/2\ (\sigma_1 - \sigma_3) > 1/2\ \sigma_n$$

assuming $\sigma_1 > \sigma_2 > \sigma_3$, and in which σ_n is the endurance limit in reversed direct stress, or in reversed flexural stress, since the value of the endurance limit should be the same in either case. An equivalent tensile stress may be defined as—

$$(23)\quad \sigma_e = (\sigma_1 - \sigma_3)$$

and hence the maximum shear stress is $\frac{\sigma_e}{2}$.

XI. THE VALUES OF STRESSES DERIVED FROM STRAIN MEASUREMENTS ON CORRUGATED PIPE.

45. *The Results of Strain Measurements.*—In order to demonstrate the application of the methods of analysis developed in the preceding sections, strain measurements were made on two corrugations of the tangent section of a quarter bend. Piece BE was erected for this test with the corrugated tangent leg vertical and measurements were made on the crests of the fourth and sixth corrugations from the bottom of the section. These corrugations were designated by the letters N and I, respectively. Two individual methods of loading were employed to produce strain. In one method a bending moment was applied to the pipe with no internal pressure, and in the other internal hydrostatic pressure was applied with no external loading or restraint. In this latter method of loading, the pipe was provided with blank flanged ends.

On each corrugation eight stations for measurements were established. These stations were placed with equal circumferential spacing along the crest of the corrugation. It was necessary to measure the longitudinal strains and hoop strains both with the bending strain gage and the tensometer at each station for each method of loading.

The results of the strain readings are pictorially tabulated in Plates XXXIV to XXXVII, inclusive. The readings reported are the result of the application of 32,750 inch-pounds or 19,650 inch-pounds bending moment or the application of 600 pounds per

square inch internal pressure as indicated on the diagrams. These values for bending moment and internal pressure have no direct connection with the fatigue tests, they were simply convenient points at which to take measurements. By applying the loading in successive increments, it was determined in each case, that the reading was proportional to the loading beyond the values reported. These readings can therefore be divided by the applied bending moment or by the applied pressure, as the case may be, and yield values of instrument reading per inch-pound applied bending moment, or pounds per square inch applied internal pressure. This scheme was employed in carrying out the calculations so that the final results for stress may be multiplied by values for moments or internal pressure to obtain stress values for the selected conditions.

46. *The Results Obtained for Values of Principal Stresses and Equivalent Stresses.*—With the methods previously described the external strain measurements were used to derive the values of the principal stresses at each of the stations on each corrugation. In the case of loading due to bending moment, $\sigma_3 = 0$, and in the case of loading due to internal pressure, $\sigma_3 = 400$ pounds per square inch. The results of the calculations for the principal stresses are tabulated below. The location of the points of measurement with reference to the pipe axes is shown in a diagram on Plate XXXVIII.

TABULATION OF PRINCIPAL STRESSES DUE TO APPLICATION OF BENDING MOMENT ONLY.

Crest of Corrugation N.

Position	*Principal Stresses in pounds per square inch per 100 inch-pounds moment*		
	σ_1	σ_2	σ_3
1	—74.3	—10.1	0
2	—62.1	—8.9	
3	—0.6	0	
4	+35.8	+3.5	
5	+48.5	+3.2	
6	+45.5	+5.9	
7	—8.0	—0.8	
8	—52.3	—6.4	

Crest of Corrugation I.

Position	*Principal Stresses in pounds per square inch per 100 inch-pounds moment*		
	σ_1	σ_2	σ_3
1	—84.3	—13.6	0
2	—49.3	—5.8	
3	+0.2	+0.8	
4	+33.6	+4.0	
5	+68.5	+14.3	
6	+33.3	+3.1	
7	+1.3	+0.6	
8	—52.5	—7.4	

It may be seen that with one exception, and this in a region of low stress, the greatest principal stress is σ_1 and the least principal stress is σ_3 at each point of measurement. The value of σ_e will therefore, from equation (23), always be equal to the value of σ_1 minus 0, in the case of loading due to bending moment, and will be equal to σ_1 minus the value of the internal pressure in the case of loading due to internal pressure. In the region of highest stress, the value of the radial stress corresponding to pressures for which the pipe was designed is small compared to the value of σ_1 and may be neglected without appreciable error. Hence for all cases it may be assumed $\sigma_e = \sigma_1$. This indicates that the hoop stresses, being of intermediate value between the longitudinal and radial stresses, have no influence on the strength of the pipe.

The value of the equivalent stress at each point of measurement, when an external bending moment was applied, is shown in Plate XXXVIII. This stress is plotted in values of pounds per square inch per 100 inch-pounds moment. Thus to obtain the equivalent stress induced by a known moment, the value from the curve should be multiplied by the value of the known moment divided by 100.

The values of the equivalent stresses caused by internal pressure only are as follows:

Crest N, $\sigma_1 = 52.4$ pounds per square inch per pound per square inch internal pressure.

Crest N, $\sigma_2 = 15.1$ pounds per square inch per pound per square inch internal pressure.

Crest N, $\sigma_e = 51.4$ pounds per square inch per pound per square inch internal pressure.

Crest I, $\sigma_1 = 40.1$ pounds per square inch per pound per square inch internal pressure.

Crest I, $\sigma_2 = 11.8$ pounds per square inch per pound per square inch internal pressure.

Crest I, $\sigma_e = 39.1$ pounds per square inch per pound per square inch internal pressure.

Thus, at the designed working pressure of this pipe; namely, 400 pounds per square inch, the maximum stress observed was over 20,000 pounds per square inch. The significance of these values for stresses caused by internal pressure will be discussed later.

As in the case of stresses caused by bending moments the intermediate stress value, the hoop stress, has no influence on strength.

XII. THE STRESS INTENSIFICATION FACTOR.

47. *The Value of Stress at the Endurance Limit.*—The endurance limit is a physical property of a metal and has a definite value. In the case of the steel used in the manufacture of the piping under investigation, the endurance limits are as follows:

Series A—25,100 pounds per square inch.
Series B—24,600 pounds per square inch.
Series C—25,300 pounds per square inch.

These values were determined as 43 per cent of the average tensile strength of the specimens in each series of pipes.

In the asymptotic portion of the endurance graphs, the stress in the metal must be at the endurance limit. The stress intensification factor has been defined as the ratio between the endurance limit and the nominal stress at this point on the fatigue graph. The values of the stress intensification factors obtained in this manner are:

Series A, $N = 8.7$
Series B, $N = 9.5$
Series C, $N = 6.1$

These values indicate that the nominal stresses have been effectively multiplied at the endurance limit by the factors indicated. It is considered that the discrepancy between the Series A and Series B pipes may partially be explained by the relatively few points available to determine the endurance limits on the fatigue graphs.

48. *The Stress Intensification Factor from Computed Stresses.*—The maximum stress shown on Plate XXXVIII appears to be at point 8 on I corrugation and has a value of 84.3 pounds per square inch per 100 inch-pounds moment. At the endurance limit, as defined on Plate XX for Series B piping, the bending moment is 23,500 inch-pounds. Hence the value of $\sigma_1$max. = 19,800 pounds per square inch. This value gives a value for stress intensification factor of 7.3. This compares with the value of 9.5 for the B series obtained from the endurance testing method.

These results are in good experimental agreement. The value of 9.5 obtained from the endurance tests is probably slightly high because it is derived from a value for endurance limit associated with tests of small, highly polished, specimens tested at high frequency. The actual steel in the pipe has a rough surface and if this surface were duplicated in a small specimen, the resulting endurance limit would undoubtedly be somewhat lower than for the highly polished specimen. The speed effect probably has no influence as such. However, if corrosion is present the rough pipe surface offers more opportunity for attack during the time of test than the polished one. The true value of the endurance limit of the metal itself as actually in the pipe is probably somewhat less than the value of 24,600 pounds per square inch. The strain measurements upon which the computed stress results are based were made over a finite gage length across a region where the strain was varying. The results, therefore, represent an average which is somewhat below the maximum. The value of the stress intensification factor computed from the stresses indicated from these measurements will probably be low. The measurements were made primarily to demonstrate the method of determining the stresses and not for the purpose of developing the stress intensification factor. The ultimate failure of this piece, BE, in fatigue test, did not occur in either of the corrugations in which the stress was measured. Examination of the pipe after the test, however, showed that the metal had begun to crack at the inner surface of the crest of one of the corrugations selected for strain measurement.

XIII. THE INFLUENCE OF INTERNAL PRESSURE.

49. *The Action of Internal Pressure in Pipes.*—It has been mentioned that variations in internal pressure may be a source of cyclic

stress. The high values of equivalent stress for moderate values of internal pressure indicate that severe stressing from this cause might occur. However, it should be noted that the highest principal stress, the longitudinal, was caused from the ends of the pipe being closed while pressure was applied. This would be equivalent to the pipe line in service with a valve in the line closed and linear expansion unrestrained.

If a pipe line carrying internal pressure is considered as having the ends open, the only stresses acting are the radial and hoop stresses. The longitudinal stresses may then be neglected. In this case, for moderate pressures, the value for σ_2 due to internal pressure added to the value for σ_2 due to bending moment would probably yield values which would still be intermediate between values of σ_1 and σ_3. This question should be investigated for each case considered. The value of σ_2 with an open end pipe under internal pressure will be somewhat different from the values obtained by experiment with a closed end pipe. If the open end condition can not be readily obtained in a test, the value of σ_2 due to internal pressure which will probably be low compared to the other stresses acting, may be computed with a sufficient degree of accuracy from the ordinary boiler formula

$$\frac{pD}{2t} = \sigma_2$$

where p = Internal pressure,
D = Diameter of pipe, and
t = Wall thickness.

It will be seen that there are many ways in which the stresses due to internal pressure may operate to affect the strength of piping. The pressure stresses may themselves be cyclic, in certain conditions they may be disregarded, in other conditions they may act as steady stresses upon which cyclic stresses due to other causes may be superimposed. This latter condition will operate to shift the position of the cyclic stress range but not its value.

In the fatigue tests of specimens AD, BE, and CF this condition was obtained. The pipe was placed under internal pressure and then the cyclic stress was imposed upon the steady stress.

50. *The Effect of Internal Pressure on Flexibility and Strength.*—Load-deflection tests made on pieces AD, BE and CF without internal pressure and with 400 pounds per square inch internal pressure showed practically no difference. The flexibility of these pipes was unaffected by the internal pressure.

These three pipe shapes were each fatigued tested with 400 pounds per square inch internal pressure. Four failures resulted from these tests. Piece AD, a corrugated U-bend, provided one failure. Piece BE, a quarter bend with creased arc and corrugated tangent leg, failed in the creased arc, was repaired by welding and later failed in the corrugated leg. Piece CF, a creased U-bend provided the fourth failure. In each case, disregarding the stresses from internal pressure and referring the failures to the proper fatigue graph for the applied nominal stresses induced by the bending moments, the points of failure lie in close proximity to the curves. These results indicate that the internal pressure had no appreciable effect on the endurance properties of the bends thus tested.

XIV. THE DETERMINATION OF LIMITING DESIGN STRESSES FOR CORRUGATED AND CREASED PIPING.

Notation.

σ_m = Constant mean stress
σ_r = Reversed stress
$\sigma_{y.p}$ = Yield Point in tension
σ_n = Endurance limit in reversed flexural stress
f = Factor of safety
N = Stress intensification factor

51. *The Method of Determining Safe Working Stresses.**—It is assumed that the piping in service will be subjected to variable stress. Any kind of direct variable stress may be resolved into a constant mean stress:

$$\sigma_m = \frac{\sigma_{max.} + \sigma_{min.}}{2}$$

and a reversed stress:

$$\sigma_r = \frac{\sigma_{max.} - \sigma_{min.}}{2}$$

* For a complete description of this method see paper by C. R. Soderberg, "Factor of Safety and Working Stress," APM-52-2 Transactions of Amer. Soc. Mech. Eng., 1930; also, "Strength of Materials," Vol. II, by Timoshenko.

From these equations it follows that—

$$(24)\quad \sigma_{max} = \sigma_m + \sigma_r$$

With σ_m as abscissa and σ_r as ordinate, a diagram such as shown in Figure 3, Plate XXIX, may be made on which any variable stress can be represented by a point in the σ_m, σ_r plane. In this diagram let A represent the yield point in a static tension test ($\sigma_r = 0$) and let B represent the endurance limit in reversed stress ($\sigma_m = 0$). It may then be assumed that the limiting stress conditions are represented by points along the line AB. If a factor of safety, f, is applied to OA and OB, points determining the line CD parallel to AB are obtained. This line represents safe stress conditions and from it may be determined safe values of σ_m and σ_r for any value of the ratio σ_r/σ_m. Referring to this Figure, the following equations result from purely geometrical considerations:

$$(25)\quad \frac{1}{f} = \frac{\sigma_r}{\sigma_n} + \frac{\sigma_m}{\sigma_{y\cdot p}}$$

$$(26)\quad \sigma_r = \frac{\sigma_n}{f} - \frac{1}{1 + \frac{\sigma_n}{\sigma_{y\cdot p}}\,\frac{\sigma_m}{\sigma_r}}$$

$$(27)\quad \sigma_m = \frac{\sigma_{y\cdot p}}{f}\,\frac{1}{1 + \frac{\sigma_{y\cdot p}}{\sigma_n}\,\frac{\sigma_r}{\sigma_m}}$$

The stress intensification factor operates to increase the nominal stress. The writer has chosen to consider that this factor operates to affect the strength of the pipe in the case of the variable stress only. In equations (25), (26) and (27) then σ_r should be replaced by $N\sigma_r$. Equations (26) and (27) then become

$$(28)\quad \sigma_r = \frac{\sigma_n}{N\,f}\,\frac{1}{1 + \frac{\sigma_n}{\sigma_{y\cdot p}}\,\frac{\sigma_m}{N\,\sigma_r}}$$

$$(29)\quad \sigma_m = \frac{\sigma_{y\cdot p}}{f}\,\frac{1}{1 + \frac{\sigma_{y\cdot p}}{\sigma_n}\,\frac{N\,\sigma_r}{\sigma_m}}$$

52. *The Method of Determining Safe Working Stresses Applied to Corrugated and Creased Pipes.*—In the great majority of prac-

tical applications a piping system will not be called upon to undergo the number of cycles of stress equivalent to that at which the endurance limit is determined. In the lifetime of an ordinary power plant, excluding serious vibration, the number of stress cycles imposed on the piping will probably be numbered in thousands rather than millions. It seems unreasonable then, in most cases, to use in design a stress value corresponding to the true endurance limit.

The true endurance limit represents the limiting value of stress to which a metal may be subjected in order to withstand an indefinitely large number of stress cycles. The fatigue graph defines this limit and also indicates the number of stress cycles to cause failure at stresses greater than the endurance limit. The value of stress taken from a fatigue graph for a stated number of cycles is here defined as the virtual endurance limit for the number of cycles selected. The definition for the stress intensification factor is extended to include the ratio of the virtual endurance limit of the steel to the virtual endurance limit of the pipe, the latter value again being expressed in terms of nominal stress. With the application limited to a stated number of cycles, the virtual endurance limit for the steel and the stress intensification factor at this virtual endurance limit may be substituted for σ_n and N in the formulas developed above.

The method used in determining the virtual endurance limits of the steel was similar to that described for determining the true endurance limits. At various selected cycle values, the stresses read from the fatigue graph of Plate VIII were expressed as certain percentages of the tensile strength of the steel used in determining that fatigue curve. These percentages were then applied to the experimentally determined tensile strengths of the pipe steel to establish the virtual endurance limits at the selected cycle values. This procedure was followed considering each series of piping individually. The stress intensification factors were then readily determined by dividing the virtual endurance limits of the steel by the virtual endurance limits of the pipe at selected cycle values. Equations (28), (29) and (24) were then solved to determine the value of the safe working stress for each series of pipes. The safe working stress was computed for two conditions; one assuming that the factor of safety was 2, and the other that the factor of safety was 1.5. The results of these computations are tabulated below:

Safe Working Stresses for Series A - Corrugated Pipe

Average tensile strength = 58400 lbs.per sq.in.
Average yield point = 38200 lbs.per sq.in.

No. of Cycles	Stress Intensification Factor N	Virtual end. Limit σ_n	Safe Working Stress for $f = 2$ σ max.	Safe Working Stress for $f = 1.5$ σ max.
$1x10^7$	8.7	25100	2680	3580
$5x10^5$	7.2	28800	3640	4840
$1x10^5$	5.2	34000	5580	7430
$5x10^4$	4.7	37500	6590	8800
$3x10^4$	4.5	40600	7300	9720
$2x10^4$	4.4	43500	7860	10460

Safe Working Stresses for Series B - Corrugated Pipe

Average Tensile Strength = 57300 lbs.per sq.in.
Average Yield Point = 39100 lbs.per sq.in.

No.of Cycles	Stress Intensification Factor N	Virtual Endurance Limit σ_n	Safe Working Stress for $f = 2$ σ max.	Safe Working Stress for $f = 1.5$ σ max.
$1x10^7$	9.5	24600	2430	3240
$5x10^5$	6.4	28300	3980	5300
$1x10^5$	4.3	33400	6480	8620
$5x10^4$	3.9	36800	7620	10160
$3x10^4$	3.8	40000	8280	11040
$2x10^4$	3.7	42600	8880	11840

Safe Working Stresses for Series C - Creased Pipe

Average Tensile Strength = 59000 lbs.per sq.in.
Average Yield Point = 40900 lbs.per sq.in.

No.of Cycles	Stress Intensification Factor N	Virtual Endurance Limit σ_n	Safe Working Stress for f = 2 σ max.	Safe Working Stress for f = 1.5 σ max.
$1x10^7$	6.1	25300	3770	5020
$5x10^5$	5.5	29000	4670	6220
$1x10^5$	4.5	34300	6430	8570
$5x10^4$	4.2	37800	7370	9820
$3x10^4$	3.9	41000	8340	11100
$2x10^4$	3.8	43800	9010	12000

These results indicate that, in general, the Series B corrugated pipe could be subjected to slightly higher safe working stresses than the Series A pipe. All pipes were manufactured with the same amplitude and pitch of corrugations. The Series B pipe, however, had a slightly greater wall thickness and a somewhat different curvature of corrugation from the Series A pipe. Typical sections of the two corrugated shapes are shown in Plate II and Figure 5 of Plate XXIX. It should be noted here that the flexibility factors for the tangent lengths of piping of each of the two series are essentially the same.

53. *The Selection of Safe Working Stresses for Design Purposes.*—The safe working stresses for each of the series of pipe may be expressed as a fractional part of the tensile strength as follows:

Ratio of Tensile Strength to Safe Working Stress

Cycles	Series A Corrugated		Series B Corrugated		Series C Creased	
	f = 2	f = 1.5	f = 2	f = 1.5	f = 2	f = 1.5
1×10^7	21.8	16.3	23.5	17.7	15.7	11.7
5×10^5	16.0	12.1	14.4	10.7	12.6	9.5
1×10^5	10.5	7.9	8.8	6.6	9.2	6.9
5×10^4	8.9	6.6	7.5	5.6	8.0	6.0
3×10^4	8.0	6.0	6.9	5.2	7.1	5.3
2×10^4	7.5	5.5	6.5	4.8	6.5	4.9

The average tensile strength for the steel used in the manufacture of the pipes tested was approximately 58,000 pounds per square inch, which is about the mean of the range of tensile strengths of steel used in ordinary commercial practice for seamless drawn steel tubing intended for high temperature service.* These ratios may then be used as a satisfactory approximation for design purposes in determining the safe working stress for pipes fabricated from tubing whose tensile strength and yield point values are within this usual commercial range.

The use of a factor of safety of 2 is considered conservative. The use of a lower value, such as 1.5 or some intermediate value, would undoubtedly be justified when it was known that the tubing material was of uniformly high quality, when the service conditions were not severe, and the values of the applied stresses could be predicted with reasonable accuracy.

Pipe shapes may successfully withstand large deflections and absorb very high applied stresses for single, or very few, applications of load. Mention has already been made of a test case where a pipe bend was completely collapsed without fracture. There may be some piping installations where the service application may involve an approximately steady loading condition. When this is

* See A. S. T. M. Specifications A-106-33T.

true the piping design may be based entirely on the static tensile properties of the metal. If, however, in the designer's opinion, the piping is to be subjected to variable stresses static strength considerations are insufficient and the design should be based on an extremely liberal allowance for the number of stress cycles to be encountered.

The fatigue graph is useful primarily for determining the safe limiting value of stress for a large number of cycles. The curve is necessarily the mean path through a number of observed points and can not be considered as applying with sufficiently close accuracy for literal application in predicting individual failures. A slight variation in stress value will cause a large percentage error in the number of cycles at any point on the curve. These considerations are particularly important in the high stress-low cycle region of the fatigue graph. The action of steel at high variable stresses and high temperatures can not be safely predicted. For these reasons the writer is of the opinion that 20,000 cycles of variable stress should be the absolute minimum basis for design purposes when cyclic stress conditions are considered, regardless of the actual predicted numerical value of the stress cycles to which the pipe may be expected to be subjected. In any case the number of cycles selected as a design basis, in accordance with the method presented, should be considerably greater than the number of cycles it is estimated the pipe will experience. This is particularly important, as has been previously indicated, in applications where corrosion is likely to be a factor.

54. *Application of Design Values to Other Sizes of Corrugated and Creased Pipes.*—Although many of the conclusions reached in this investigation are of general application, the values given for flexibility factors and for limiting design stresses will not be strictly applicable where piping is being considered which departs from geometrical similarity with the pipes tested. A flexibility factor value of between 5 and 6 will probably closely fit any usual corrugated pipe. The true value, however, can easily be determined by simple experiment.

Where piping sizes or creased or corrugated shapes are being considered whose dimensions are such as to make the factors for determination of safe working stresses here given of doubtful ap-

plication, the methods of stress determination based on strain measurement may be applied. For this purpose the dimensions of the pipe and corrugations or creases must be known.

Since the critical zone of failure in a creased pipe is on the outer wall surface the strain measurement method which has been described as applying to a corrugated pipe, may here be more simply applied. After readings with the bending strain gage and with the tensometer have been obtained, these values are used in connection with equations (1), (2), (16) and (17) to obtain results for the resultant longitudinal and hoop strains. The principal stresses and equivalent stress may then be determined in a manner similar to that described for the case of a corrugated pipe.

The yield point and tensile strength of the steel may be easily determined. A value of the virtual endurance limit for the steel is then selected, as has been described, for the desired number of cycles. Equations (24), (26) and (27) are then employed to determine the value for the safe working stress. The remaining step is to determine what loads, or deflections, will produce a value of the equivalent stress equal to this safe working stress.

XV. CONCLUSIONS.

55. *The Flexibility of Corrugated and Creased Bend Pipes.*— The load-deflection characteristics for each of the three series of corrugated and creased bend pipes are presented in Plates XIII to XVII. The flexibility factor for the corrugated tangents was found to be approximately 6. The corrugated arc compared to a theoretical smooth pipe arc of the same major dimensions had a relative flexibility advantage of 2.6 to 1. The corrugated arc compared to a smooth pipe arc is relatively less flexible than the corrugated tangent compared to a smooth pipe tangent because of the increased flexibility of a smooth pipe arc due to the flattening effect.

The creased bends had a relative flexibility compared to a theoretical smooth pipe bend of 1.3 to 1. Both the corrugated arc and the creased bend, however, were curved to a smaller radius of curvature than would be practicable for an actual smooth pipe bend.

The flexibility of both corrugated and creased pipes appeared to be unaffected by 400 pounds per square inch internal hydrostatic pressure.

56. *The Endurance Properties of the Pipes Under Variable Stresses.*—The results of the fatigue tests on each of the series of pipes are shown in Plates XIX to XXI, inclusive. Internal hydrostatic pressure of 400 pounds per square inch was applied to three pipes tested under cyclic stress and appeared to have no effect on the strength of the pipes.

The stress intensification factors at the endurance limits of the pipes were found to be—

$$\text{Series A, } N = 8.7$$
$$\text{Series B, } N = 9.5$$
$$\text{Series C, } N = 6.1$$

These results indicate that, at the endurance limit of the pipes, the nominal stresses which were computed for the given loading on a hypothetical smooth-walled pipe of the same basic dimensions as the pipes tested, were effectively multiplied by these factors. The values of the stress intensification factors for cycle values below the endurance limit are tabulated in section 52.

With one exception all fatigue failures in corrugated pipe developed from cracks which started from the inside surface of the pipe and worked outwards. The failures all occurred in the crest of the corrugations. The single exception concerned the failure of an expansion U-bend which failed from the outside between two corrugations, due probably to severe crimping of the pipe on the inner side of the arc where failure occurred, during fabrication.

Without exception all crease-bend failures occurred from cracks which developed from the outside pipe surface. These failures all occurred in the crease.

The nature of the failure occurring in the corrugated pipes indicates that it is unlikely that the ultimate fracture would be anticipated by the appearance of surface cracks on the outside of the pipe.

57. *The Measurement of Strains and the Determination of Stresses.*—A method is presented for measuring the bending strains and resultant strains on the outside of a corrugated pipe, and from these measurements to determine the strains on the inside surface of the pipe. The strains on the inside of these pipes are of greatest interest because of the indication from the fatigue tests that failure starts from this surface. It is further demonstrated how the prin-

cipal stresses may be determined from the strains. The maximum-shear theory is considered to apply to fatigue failures of pipes. The longitudinal stress, in general, appears to be the maximum principal stress on the inner surface of the corrugated pipe at the zone of failure of the radial stress the minimum principal stress. In most cases the hoop stress, being of intermediate value, will not affect the strength of the pipe. An investigation of the stresses caused by internal pressure indicated that, as confirmed by fatigue experiments, the internal pressure should have little or no effect on the ability of the pipes to withstand cyclic stresses.

58. *The Derivation of Safe Working Stresses.*—A method of determining safe working stresses based on the endurance limit and the yield point is presented. The method was applied to each of the series of pipes and results tabulated in section 52. Safe working stresses were determined using the true endurance limit and also using a virtual endurance limit as a basis. The use of this latter value yielded results for safe working stresses for various selected values of the number of stress cycles to which the pipe would be subjected.

For design purposes a tabulation is presented in section 53 from which, given the tensile strength of usual commercial seamless-drawn tubing, the safe working stresses for this tubing in the form of corrugated or creased pipes may be closely approximated.

It is considered that, if cyclic stress considerations are to enter into the design of pipe, 20,000 cycles of stress should be the absolute minimum used as a basis for design regardless of the actual predicted numerical value of the stress cycles which the pipe may be expected to experience. In any case the number of cycles selected as a design basis should be considerably greater than the number of cycles it is estimated the pipe will experience. This is highly important in applications where corrosion is likely to be a factor. A method is presented for determining safe working stresses for pipe shapes or sizes which deviate sufficiently from the pipes herein investigated to cause the factors presented to be of questionable suitability. This method involves the strain measurement methods presented.

59. *General Summary.*—The use of corrugated and creased pipe offers two principal advantages; the forces exerted against the

anchor points by pipe expansion are low, and the pipe may be bent to much smaller radii of curvature than is practicable for smooth-walled pipe. However, the factors which operate to increase the flexibility of these pipes in turn operate to increase the stress. This increase of stress may more than counterbalance the effect of increased flexibility.

It is essential that, since these pipe shapes involve areas of highly localized stress, the tubing from which the pipes are fabricated should be of uniformly high quality.

The primary objects of the investigation, stated in the Introduction, have been accomplished. The inherent complexity of the problem has made it impracticable to develop a general method for the determination of safe working stresses which will relieve the pipe designer from the necessity for exercising judgment. Methods have been developed, however, and factors presented which when properly applied should lead to a safe and satisfactory design of piping systems which include the corrugated and creased bend pipes.

APPENDIX.

I.

60. *Calculation of Bending Moments Due to Expansion in a Single Offset Quarter Bend.*—The calculations herein presented are for the purpose of illustrating the application of methods which have been adequately explained elsewhere.* For illustrative purposes the single offset quarter bend, piece AM, Plate III, has been selected. This bend is unsymmetrical and includes arcs of less than 90 degrees.

The purpose of the calculations is, for assumed conditions, to determine the bending moments at various parts of the bend. When the bending moments are determined, the value of the nominal stress at the point of maximum moment or at any other point may readily be calculated.

In this example the bend is assumed to be installed with the end flanges fixed. The bend is then considered to be heated. The anchor at one end of the bend is replaced by the forces necessary

* Piping Handbook by Walker and Crocker; discussion by A. E. R. de Jonge, of "Frictional Resistance and Flexibility of Seamless Tube Fittings Used in Pipe Welding," by Crocker and McCutchan, FSP-53-17, A. S. M. E. Trans., 1931. Also, Appendix IV to "Load-Deflection Relations for Large, Plain, Corrugated and Creased Pipe Bends," by Cope and Wert, FSP-54-12, A. S. M. E. Trans., 1932.

to maintain the flange in its fixed position. Figure 1 of Plate XLIII shows a diagrammatic dimensioned sketch illustrating this condition.

The following assumptions are made:

Temperature rise of pipe = 400 degrees F., from 32 degrees F.

$E = 30 \times 10^6$ pounds per square inch at 32 degrees F.

Outside diameter of basic pipe = 6.125 inches.

Inside diameter of basic pipe = 5.779 inches.

Dimensions of the bend are as shown in Figure 1, Plate XLIII.

Modulus of Elasticity at 432 degrees F.

$$E_t = E_{32} \left[1 - \left(\frac{t - 32}{1700}\right)^2\right]^*$$

(30) $E_t = 30 \times 10^6 \times 0.945 = 28.35 \times 10^6$ pounds per square inch.

Linear Expansion at 432 degrees F.

From the formula of Holborn and Day (Mark's Handbook, 2nd Ed., pg. 300):

$$l = l_o \left[1 + a \left(\frac{t - 32}{1000}\right) + b \left(\frac{t - 32}{1000}\right)^2\right]$$

where l = length of metal at temperature t.

l_o = length of metal at 32 degrees F.

$a = .006212$ for steel

$b = .001623$ for steel

Hence the inches increase in length per inch of metal at 400 degrees F. would be:

(31) $1 = 2746 \times 10^{-6}$ inches

The Rigidity Multiplication Factor for a Smooth Pipe of Equivalent Basic Dimensions.

$$K = \frac{10 + 12\lambda^2}{1 + 12\lambda^2}$$

$$\lambda = \frac{tR}{r^2}$$

---

* "High Pressure Steam Boilers," by G. A. Orrok, A. S. M. E. Trans., 1928.

where t = wall thickness in inches = 0.173
R = radius of arc in inches = 15
r = mean radius of pipe in inches = 2.976
λ = 0.293

and

(32) K = 5.433

The Moment of Inertia and the Section Modulus.

$$I = \frac{\pi}{64} (D^4 - d^4)$$

(33) I = 14.33

The section modulus, I/c, is equal to the above value of the moment of inertia divided by the mean pipe radius 3.063 and has the value of 4.68.

Figure 2 of Plate XLIII represents the bend broken up into its elements, with the force Fy acting. The moment diagram resulting from the application of this force is shown in Figure 3. The area enclosed in the dotted lines represents the resisting moment due to the fixed end assumption. The ordinate, 31.4 F, is equal to the net area of the bending moment diagram due to Fy, divided by the length of the diagram. The determination of the value of this ordinate presupposes a knowledge of the value of V, the flexibility factor. This factor has been developed for standard shapes as explained in sections 27 to 31. The corrugation shape in this bend differed somewhat from the others tested and the flexibility factor, as will be shown, was determined by actual experiment on this bend. The case numbers on Figure 3 refer to Plates XXXIX and XL. These plates contain diagrams taken from sources previously mentioned.* Plate XLI contains curves of deflection factors to be used in connection with Plate XL.

Calculation for $\delta y = f(F_y)$ [Figure 3, Plate XLIII].

$EI\delta_{yc} = A_b \times 1 = 413\ F \times 3.3$

(From rotation) 1 363 F Up

$EI\delta_{ym}$ = Case XIII = 344.3 VF $\times$ .145

$\times$ 15 (from moment) 749 VF Up

* Piping Handbook and A. S. M. E. Transactions FSP-54-12 loc. cit.

$EI\delta_{yf}$ = Case XI = 22.5 VF × .180 × 15 (From force)			61 VF Down
$EI\delta_{yd} = A_c \times 1 - (413\ F + 321.8\ VF)\ 3.3$	1	363	F Up
	1	005	VF Up
$EI\delta_{ym}$ = Case XVI = 378 VF × .077 × 15		291	VF Up
$EI\delta_{yf}$ = Case XIV = 11.6 VF × .135 × 15		24	VF Down
$EI\delta_{ye} = A_d \times 1 = (413\ F + 688.2\ VF)\ 15$	6	195	F Down
	10	323	VF Down
$EI\delta_{ym}$ = 518.5 VF × .637 × 15	5	000	VF Down
$EI\delta_{yf}$ = Case V = 225 VF × .785 × 15	2	655	VF Down
$EI\delta_{yf} = A \times 1 - (413\ F + 1432\ VF)\ 18$	7	434	F Down
	25	776	VF Down
$EI\delta_{ym}$ = 72 F × 9		648	F Down
$EI\delta_{yf}$ = 162 F × 12	1	944	F Down

The summation of $EI\delta_y$ gives, in the down direction—

(34) $\Sigma EI\delta_y = 13{,}495 + 41{,}794\ VF$

Plate XLII shows the load-deflection relationship for this bend to be $\delta_y = 0.9 \times 10^{-3}\ F$ for an applied downward force. This measurement was made at room temperature for which $E = 30 \times 10^6$. Substituting this value of E and the experimental value of δ_y in 34, a value for V is obtained which is independent of pipe temperatures.

(35) $V = 8.935$.

It is interesting to note here from the previously computed value for K (eq. 32) that $V/K = 1.64$ or this bend is 64 per cent more flexible than a theoretical smooth pipe of the same dimensions bent to the same arc radius.

then

(36) $\delta_y = \frac{952.0}{10^6} F_y$ (From 35, 30 and 33 in 34)

Calculation for $\delta_x = f(F_y)$ [Figure 3, Plate XLIII].

$EI\delta_{xb} = A \times 1/2 = 413\ F \times 6.8$	2	808	F Right
$EI\delta_{xc} = A_b \times 9.44 = 413\ F \times 9.44$	3	899	F Right
$EI\delta_{xf}$ = Case XI = 22.5 VF × .375 × 15		127	VF Left

$EI\delta_{xm}$ = Case XIII = 344.3 × .301 × 15 — 1 554 VF Right
$EI\delta_{xd} = A_c \times 1$ = (413 F + 321.8 VF) 9.44 — 3 899 F Right
3 038 VF Right
$EI\delta_{xf}$ = Case XIV = 11.63 VF × .490 × 15 — 086 VF Left
$EI\delta_{xm}$ = Case XVI = 378 VF × .330 × 15 — 1 871 VF Right
$EI\delta_{xe} = A_d \times 1$ = (413 F + 688.2 VF) 15 — 6 195 F Right
10 323 VF Right
$EI\delta_{xf}$ = 225 VF × .5 × 15 — 1 688 VF Right
$EI\delta_{xm}$ = 518.5 VF × .363 × 15 — 2 833 VF Right

The summation of $EI\delta_x$ gives to the right

(37) $\Sigma EI\delta_x = 16{,}801\ F + 21{,}094\ VF$

Hence,

(38) $\delta_x = \frac{505.3}{10^6} F_y$ (From 35, 30 and 33 in 37).

Figure 3 of Plate XLIII shows this bend broken up into its elements and acted upon by the force F_x. Figure 5 is the moment diagram resulting from this force. The area enclosed by dotted lines is again the value of restraining moment.

Calculations for $\delta_x = f(F_x)$ [Figure 5, Plate XLIII].

$EI\delta_{xf} = A_f \times 21/3 = 92.48\ F \times 9.07$ — 839 F Left
$EI\delta_{xm} = A_m \times 1/2 = 460.8 \times 13.6\ F$ — 3 133 F
$EI\delta_{xe} = A \times 1 = 553 \times 9.44$ — 5 220 F
$EI\delta_{xf}$ = Case XII = $A_f \times .415\ R$ = 46.31 VF × .415 × 15 — 288 VF
$EI\delta_{xm}$ = Case XIII = $A_m \times .301 \times R$ = 249.6 VF × .301 × R — 1 127 VF
$EI\delta_{xd} = A_c \times 1$ = (295.9 VF + 553.3 F) 9.44 — 2 793 VF
5 223 F
$EI\delta_{xf}$ = Case XV = $A_f \times .433 \times R$ = 50.18 VF × .433 × 15 — 326 VF
$EI\delta_{xm}$ = Case XVI = $A_m \times .330 \times R$ = 153.2 VF × .33 × 15 — 758 VF

$EI\delta_{xe} = A_d \times 1 = (499.3\ VF + 553.3\ F)\ 15$ 7 490 VF
8 300 F

$EI\delta_{xf} = A \times .624 \times R = 128.25\ VF \times .624 \times 15$ 1 200 VF

A summation of $EI\delta_x$ gives to the left

(39) $\Sigma EI\delta_x = 22{,}715\ F + 13{,}982\ VF$

then

(40) $\delta_x = \frac{363.4}{10^6} F_x$ (From 30, 33 and 35 in 39)

Calculations for $\delta_y = f\ (Fx)$

$EI\delta_{ye} = A_b \times 1 = 553.3\ F \times 3.3$ 1 826 F Down

$EI\delta_{yf}$ = Case XII = $A \times .195 \times R = 46.31\ VF \times .195 \times 15$ 136 VF Down

$EI\delta_{ym}$ = Case XIII = $A \times .145 \times R = 249.6 \times .145 \times 15$ 543 VF Down

$EI\delta_{yd} = A_c \times I = (295.9\ VF + 553.3\ F) \times 3.3$
977 VF Down
1 826 F Down

$EI\delta_{yf}$ = Case XV = $50.18\ VF \times .115 \times 15$ 087 VF Down

$EI\delta_{ym}$ = Case XVI = $153.2\ VF \times .077 \times 15$ 177 VF Down

$EI\delta_{ye} = A_d \times 1 = (499.3\ VF + 553.3\ F)\ 15$
7 490 VF Up
8 300 F Up

$EI\delta_{yf} = 128.3\ VF \times .876 \times 15$ 1 686 VF Up

$EI\delta_{yg} = A_e \times 1 = (627.6\ VF + 553.3\ F)\ 22$
13 807 VF Up
12 173 F Up

A summation of $EI\delta_y$ gives, in the up direction

(41) $\Sigma EI\delta_y = 16{,}821\ F + 21{,}063\ VF$

then

(42) $\delta_y = \frac{504.6}{10^6} F_x$ (From 30, 33 and 35 in 41)

Adopting the convention that directions upwards and to the right are positive

$$(43)\quad \delta_x = \frac{363.4}{10^6} F_x - \frac{505.3}{10^6} F_y \text{ (From 38 and 40)}$$

$$(44)\quad \delta_y = -\frac{504.6}{10^6} F_x + \frac{952}{10^6} F_y \text{ (From 36 and 42)}$$

If the bend is assumed to be heated to 432 degrees F., the deflections to be forced back into the bend are the vertical length of the bend in the direction times the coefficient of expansion of steel at 432 degrees F. and the horizontal length of the bend in the x direction times the same coefficient.

$$(45)\quad \delta_x = 34.25 \times 2746 \times 10^{-6} = 94{,}050 \times 10^{-6}$$
(From 31)

$$(46)\quad \delta_y = 47.5 \times 2746 \times 10^{-6} = 130{,}400 \times 10^{-6}$$
(From 31)

Then

$$(47)\quad 94{,}050 = 363.4\, F_x - 505.3\, F_y \text{ (From 45 in 43)}$$

$$(48)\quad 130{,}400 = -504.6\, F_x + 952.0\, F_y \text{ (From 46 in 44)}$$

Solving these equations as a simultaneous system—

$$(49)\quad F_x = 1716$$

$$(50)\quad F_y = 1046$$

These are the forces exerted by the pipe against the anchor. Hence the reactive forces which are exerted on the pipe are:—

$$(51)\quad F_x = -1716$$

$$(52)\quad F_y = -1046$$

The ordinates of the bending moment diagrams, Figures 3 and 5, Plate XLIII, represent the values of the moments in terms of the applied forces. Since these Figures are not drawn to scale and are illustrative only, the curves joining the ends of the ordinates are not exact. The values of the bending moments are defined from these Figures only at the points of beginning and ending of the elements of the bend.

Moments Due to F_y—From Figure 3, Plate XLIII

Position	F_y	*Net Ordinate*	*Bending Moment*
a	—1046	—1	+1046
b		—1	+1046
c		+2.3	—2406
d		+5.6	—5858
e		—9.4	+9832
f		—27.4	+28,660
g		—31.4	+32,844

Moments Due to F_x—From Figure 5, Plate XLIII

Position	F_x	*Net Ordinate*	*Bending Moment*
a	—1716	—33.13	+56,851
b		—19.53	+33,513
c		—10.13	+17,383
d		—0.53	+909
e		+14.37	—24,659
f		+14.37	—24,659
g		+14.37	—24,659

These Bending Moments due to F_x and F_y are then combined

Position	*Total Moment*
a	+57,900
b	+34,600
c	+16,000
d	—4750
e	—14,800
f	+4000
g	+8180

The values of these moments have been plotted against the value of the developed length of the bend as shown in Plate XLIV. From this diagram it will be seen that the maximum moment at the bend is at point a and that the maximum moment in a corrugated section is at point b. The minimum moment lies between points d and e.

The nominal stresses may be computed from the bending formula

$$S = \frac{Mc}{I}$$

or at point a

$$S = \frac{57,900}{4.68} = 12,400 \text{ pounds per square inch}$$

and at point b

$$S = \frac{34,600}{4.68} = 7390 \text{ pounds per square inch.}$$

The nominal stresses at any other point on the bend may be computed in a similar manner using the proper value for the bending moment, selected from the curve of Plate XLIV.

ACKNOWLEDGMENTS.

The work upon which this dissertation is based was undertaken at the U. S. Naval Engineering Experimental Station, Annapolis, Maryland, under the authorization and direction of the Bureau of Engineering of the Navy Department. The writer wishes to acknowledge his indebtedness to Captain O. L. Cox, U. S. Navy, Director of the Experiment Station, for his active interest and constant encouragement in carrying out the investigation.

The writer also wishes to take this opportunity to express his thanks to others who have aided him. Mr. W. C. Stewart, Metallurgist, has contributed many valuable suggestions and has given much helpful advice. Dr. W. M. Coates, Associate Professor of Mathematics and Mechanics at the U. S. Naval Postgraduate School, has contributed valuable criticism. He suggested the method of measuring bending strains in the pipe and has kindly permitted the writer to refer to his unpublished monograph on stress distribution in shells. Mr. B. F. Treat, Associate Mechanical Engineer, has contributed helpful suggestions and assisted in designing the fatigue testing machines and in checking the computations. Mr. J. D. Irons, Junior Metallurgist, and Mr. R. W. Reynolds, Under Engineering Aide, performed excellent work in observing many of the

experimental data. Mr. J. B. Lincoln, Senior Mechanical Engineer, has also contributed valuable suggestions.

Appreciation and gratitude are due Professor A. G. Christie, Department of Mechanical Engineering, of the Johns Hopkins University, for his inspiring instruction in engineering, and for his helpful interest and criticism in connection with this investigation.

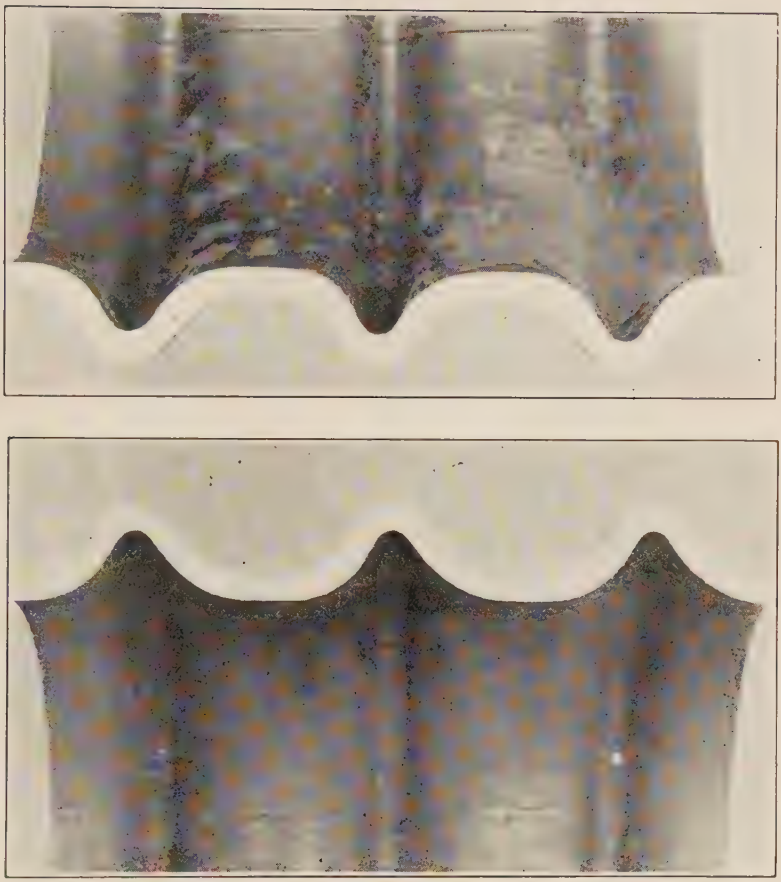

PLATE I.

FIG. 1 (AT BOTTOM)—LONGITUDINAL SECTION SHOWING A PROFILE OF TYPICAL CORRUGATIONS IN SERIES A PIPING.

Note the slightly different curvatures of the corrugations at the inner pipe surface.

FIG. 2 (AT TOP)—LONGITUDINAL SECTION SHOWING A PROFILE OF TYPICAL CORRUGATIONS IN SERIES B PIPING.

Note here also the lack of exact similarity in the corrugation.

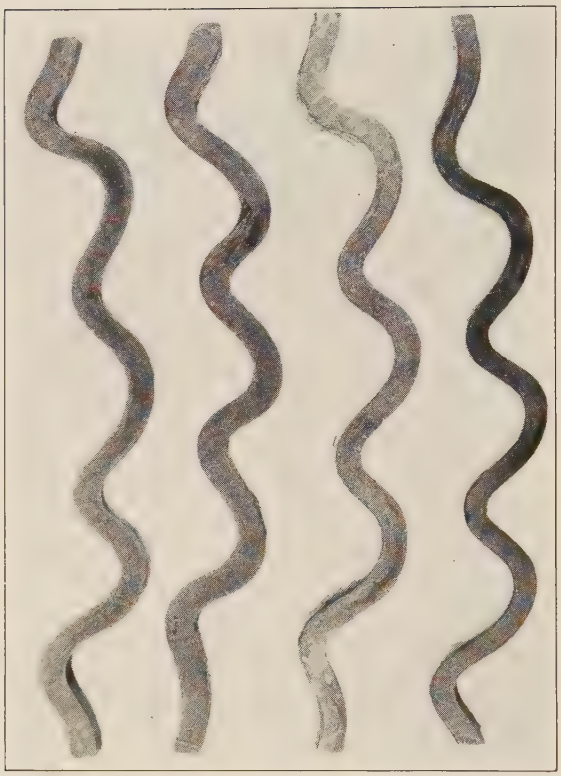

PLATE II—LONGITUDINAL STRIPS CUT FROM THE PLANE OF BENDING IN A CREASED-BEND.

These strips were cut from piece CD, an expansion U-bend. Each strip represents half an arc length of each of the four creased arcs. In this photograph the inner pipe surface is at the right of each strip. Note the individual character of the creases.

Type Bend	Designation	Sketch	Dimensions R	A	B	C	D	Class Steel A.S.T.M. Spec. A 106-33 T	Physical Properties: Tensile Strength	Yield Point	Elongation % 1 in.	Elongation % 2 in.	Red Area %	Chemical Analysis: C	S	P	Mn	Si	Heat Treatment (See Note)
Straight Tangent	AA			6'-3⅜"	5'-9⅞"			A	51,500	35,500	62	43	67						Normalized
	AB			6'-4⅜"	5'-8⅛"			A	51,650	34,350	62	42	68.4	0.13	0.024	0.011	0.53	0.01	Stress Relieved
	AC			6'-5"	5'-8"			B	66,200	43,900	51	36	43.9	0.27	0.029	0.014	0.56	0.073	Normalized
Expansion U-Bend	AD		1'-9"	8'-6⅜"	4'-1⅛"	4'-0½"		A	58,000	35,350	64	43.5	63.1						Normalized
	AE		1'-9"	8'-6⅜"	4'-0½"	4'-0½"		B	70,000	43,000		36	46						Normalized
	AF		1'-9"	8'-6⅜"	4'-0½"	3'-11⅛"		A	56,700	38,100	64	43.5	65.9	0.16	0.022	0.015	0.54	0.10	Stress Relieved
Quarter Bend with Tangents	AG		1'-9"	5'-3⅜"	5'-3⅜"			A	52,300	33,400	51	33	62.9	0.13	0.024	0.011	0.53	0.01	Normalized
	AH		1'-9"	5'-3⅜"	5'-3⅜"			A	51 600	37,300	68	48	72.6						Stress Relieved
Straight Tangent (Plain Ends)	AJ			13'-10"	3'-4"			A	60,000	34,900		41.7							Stress Relieved
	AK			13-9⅞"	3'-4"			A	61 250	40,000		39							Stress Relieved
	AL			13'-10"	3'-10"			A	61,500	42,000	60	41.5	61						Stress Relieved
Single Offset Quarter Bend	AM		1'-4"	3'-11⅛"	2'-4"	1'-0½"	1'-6¼"												
			Special Semi-Corrugated Bend 6.125 in OD × 0.173 in. Wall Thickness																

All Pipe - Seamless Steel Tubing
6.625 in O.D. × .280 in Wall Thickness
Pitch of Corrugations - 2½ in
Amplitude of Corrugations - ¼ in

Note - Heat Treatment
Normalized - 1575°F for 30 min. Cooled in Air
Stress Relieved - 1200°F for 30 min. Cooled in Furnace

PLATE III—MATERIAL LIST FOR SERIES A PIPING.

Type Bend	Designation	Sketch	Dimensions R	A	B	C	D	Class Steel A.S.T.M. Spec A-106-33 T	Physical Properties Tensile Strength	Yield Point	Elongation % 1 in	Elongation % 2 in	Red. Area %	Chemical Analysis C	S	P	Mn	Si	Heat Treatment (See Note)
Straight Tangent	BA			6'-3 3/4"	4'-9"			A	53,800	37,200	48.0	35.8	33.3						Stress Relieved
	BB			6'-3 3/8"	4'-11 1/8"			A	53,800	37,200	48.0	35.8	33.5	0.14	0.029	0.012	0.39	0.01	Stress Relieved
	BC			6'-4"	4'-10 5/8"			A	53,800	37,200	48.0	35.8	33.5						Stress Relieved
Quarter Bend with Tangents	BD			1'-3"	5'-3"	5'-3"		A	55,300	37,400	55.0	42.0	54.8						Stress Relieved
	BE			1'-3"	5'-3"	5'-2 5/8"		A	53,750	38,300	58.0	36.5	67.4						Stress Relieved
	BF			1'-3"	5'-3"	5'-3"		A	53,750	38,300	58.0	36.5	67.4						Stress Relieved
Straight Tangent (Plain Ends)	BG			13'-10"	3'-4"			A	61,100	42,100	61.0	41.0	63.4						Tempered
	BH			13'-10"	3'-4"			A	72,600	46,000		25.5	75.1	0.17	0.024	0.015	0.64	0.15	Tempered
	BJ			13'-10"	3'-4"			A	57,500	38,300	59.0	37.5	59.8						Stress Relieved
Quarter Bend with Tangents	CA			1'-3"	5'-3"	5'-3"		A	59,900	41,900		41.0	66.1	0.16	0.022	0.015	0.64	0.15	Stress Relieved
	CB			1'-3"	5'-3"	5'-3"		A	53,800	35,250		40.2	60.0						Stress Relieved
	CC			1'-3"	5'-3"	5'-3"		A	56,500	40,000	60.0	39.0	61.7						Stress Relieved
Expansion U-Bend	CD	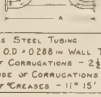		1'-3"	8'-5 3/4"	3'-11 3/8"	4'-0 1/2"	0'-11 3/4"	A	63,000	42,100		32.8	68.6						Stress Relieved
	CE			1'-3"	8'-6 1/4"	4'-0 3/8"	4'-0 1/2"	1'-0"	A	60,000	43,700	59.0	42.0	66.9						Stress Relieved
	CF			1'-3"	8'-6 1/4"	4'-0"	4'-0"	1'-0 1/8"	A	60,500	42,300	46.0	30.5	60.6						Stress Relieved

All Pipe - Seamless Steel Tubing
6.625 in O.D. × .0288 in Wall Thickness
Pitch of Corrugations - 2½ in.
Amplitude of Corrugations - ¾ in.
Pitch of Creases - 11° 15' approx.

Note - Heat Treatment
Stress Relieved - Heated to 1200°F for 18 min. Cooled in Air.
Tempered - Heated to 1800°F. Quenched in Water
Reheated to 1200°F. Cooled in Air

PLATE IV—MATERIAL LIST FOR SERIES B PIPING.

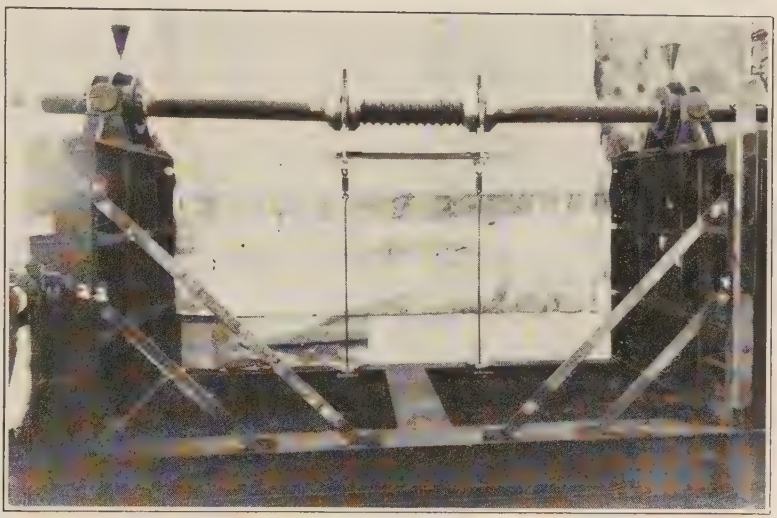

PLATE V—THE ROTATING BEAM TESTING MACHINE.

This machine was designed to apply a constant loading, or specific stress, to the pipe specimen. The pipe was rotated about its axis by a belt drive. A desired amount of dead weight load could be applied on the hangers shown below each journal at the ends of the corrugated section. Note the six-foot scale extended below the corrugated pipe section.

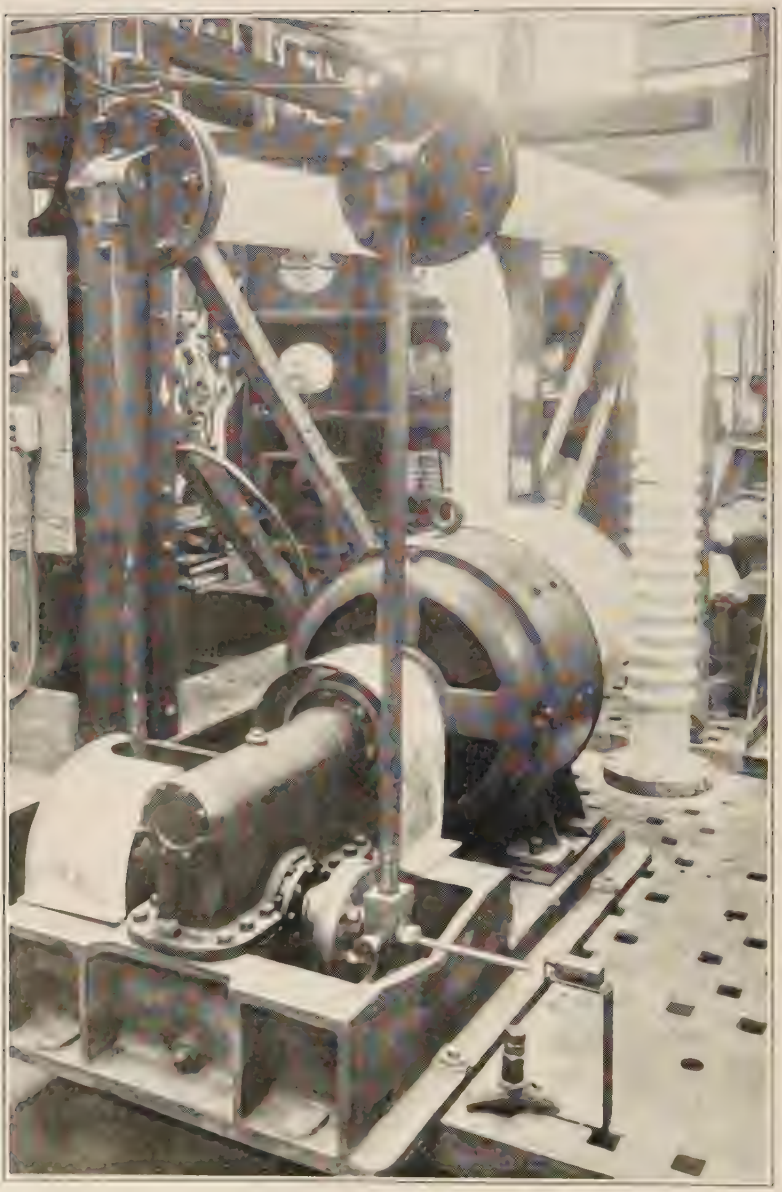

PLATE VI—TWO QUARTER-BENDS ERECTED FOR TEST ON THE MOTOR DRIVEN SPECIFIC STRAIN TESTING MACHINE.

The motor drove, through reduction gearing, two cranks mounted on eccentrics. The eccentrics were adjustable to produce the desired amount of deflection of the pipes.

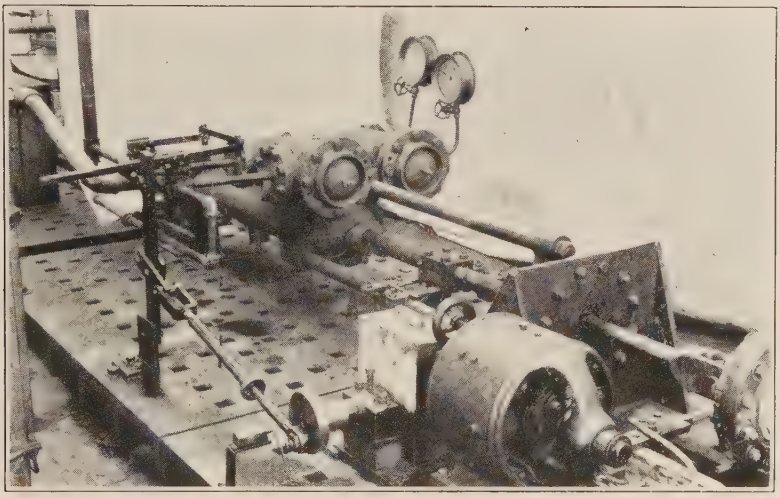

PLATE VII—PUMP DRIVEN SPECIFIC STRAIN TYPE TESTING MACHINE.

This machine was developed from the water end of a reciprocating pump. A hydraulic system, under pressure, was connected to either end of the pump cylinder. The water was alternately admitted to one end of the cylinder and discharged from the other through an arrangement of plug cocks. The plug cocks were operated by a motor driven through linkages, shown in foreground. A flange of a pipe specimen under test may be seen in the lower right of the photograph, attached to the end of the pump rod. The movement of the rod was controlled by suitable adjustment of the plug cock linkage and by stops applied to the rod. The cycle frequency was about 20 per minute.

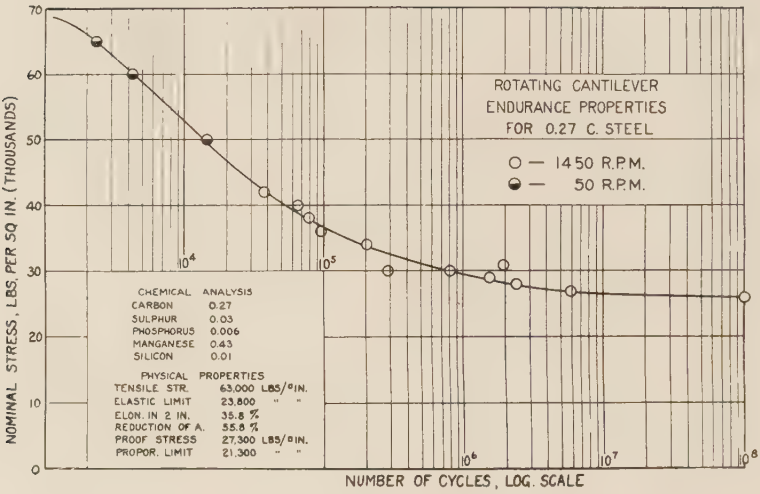

Plate VIII—Fatigue Graph for a Low Carbon Steel Similar to the Steel Used in the Manufacture of the Pipe Under Test.

The ordinate scale represents the value of the applied bending stress and the abscissa scale represents the number of cycles. The points on the graph indicate failures of specimens. Rotating cantilever specimens were used. These specimens had a conically tapered test length and a maximum diameter in the region of highest stress of about one-half inch.

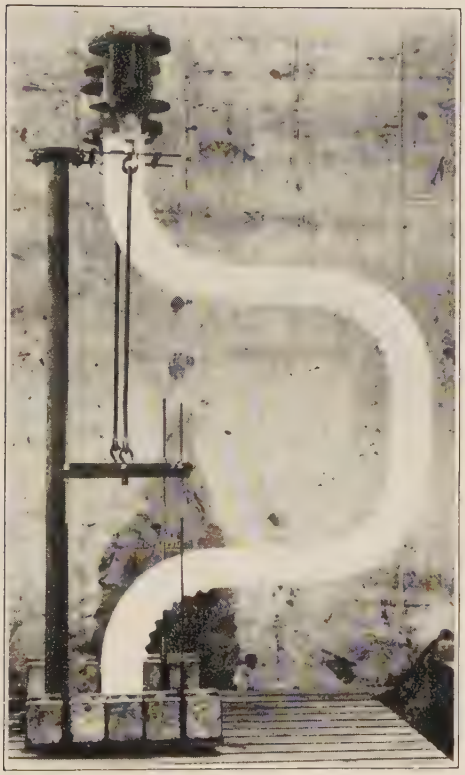

PLATE IX—AN EXPANSION U-BEND ERECTED FOR LOAD-DEFLECTION MEASUREMENTS IN THE FREE END CONDITION.

The deflections were measured from the top flange to the fixed framework mounted just below it. The loads were hung on pivoted supports from a cross-piece.

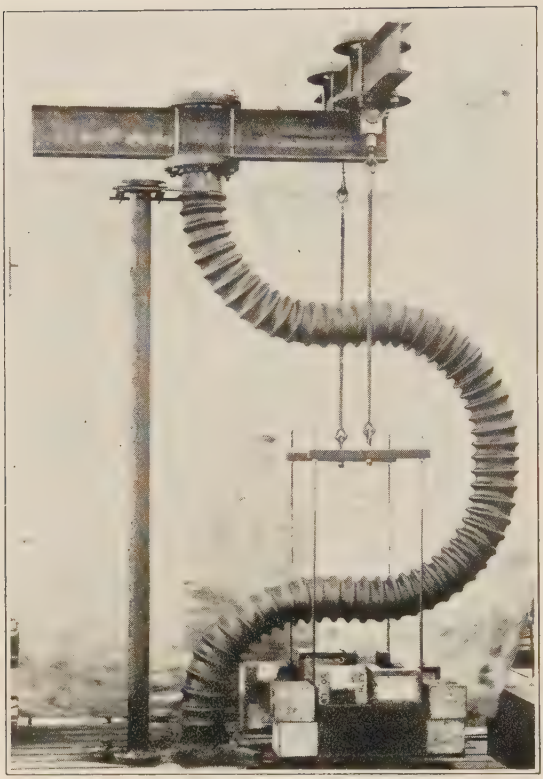

PLATE X—AN EXPANSION U-BEND ERECTED FOR LOAD-DEFLECTION MEASUREMENTS IN THE FIXED END CONDITION.

The moment arm from the center of the top flange to the line of action of the applied dead-weight load was adjusted so that the top flange always remained horizontal as increasing loads were applied. This condition was checked by a spirit level (not shown) mounted on the top flange. The deflections were measured from the top flange to a fixed framework just under the flange.

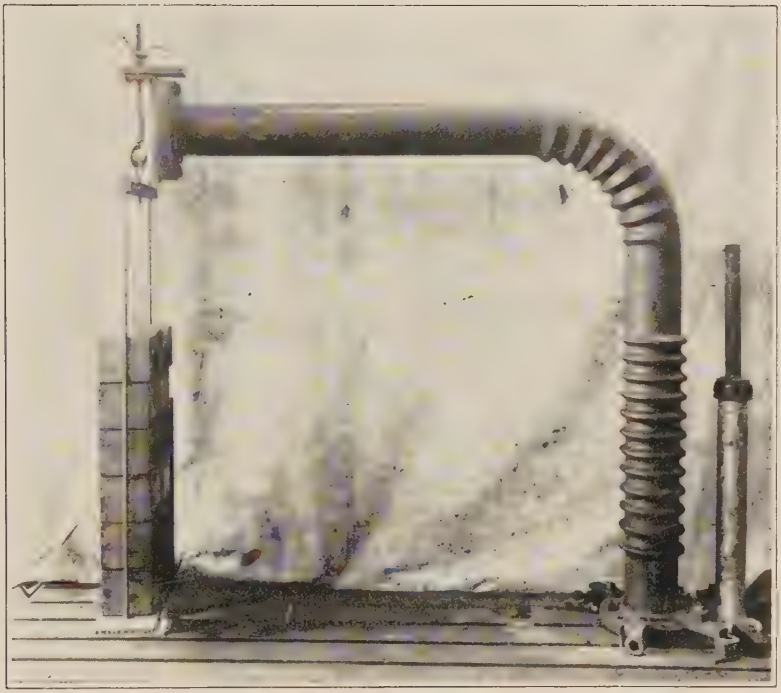

PLATE XI—A QUARTER-BEND ERECTED FOR LOAD-DEFLECTION MEASUREMENTS.

The deflections were measured from the bottom of the free flange to a fixed batten mounted just below it. Standard weights were supported in a pan hung from the free flange.

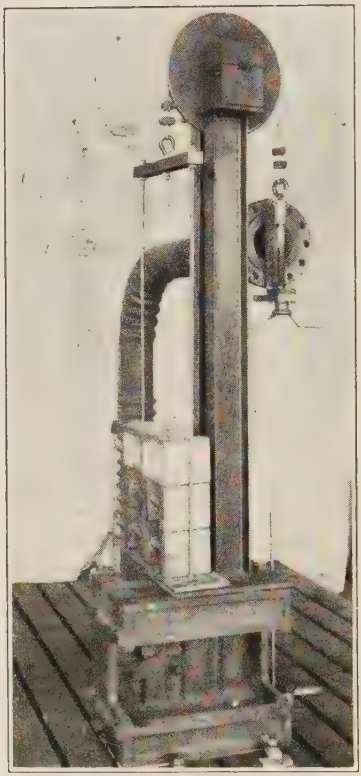

PLATE XII—A QUARTER-BEND ERECTED FOR LOAD-DEFLECTION MEASUREMENTS WITH THE LOADING APPLIED UPWARDS.

The deflections were measured from the free flange to a fixed batten. Standard weights were supported in a pan to apply the loading.

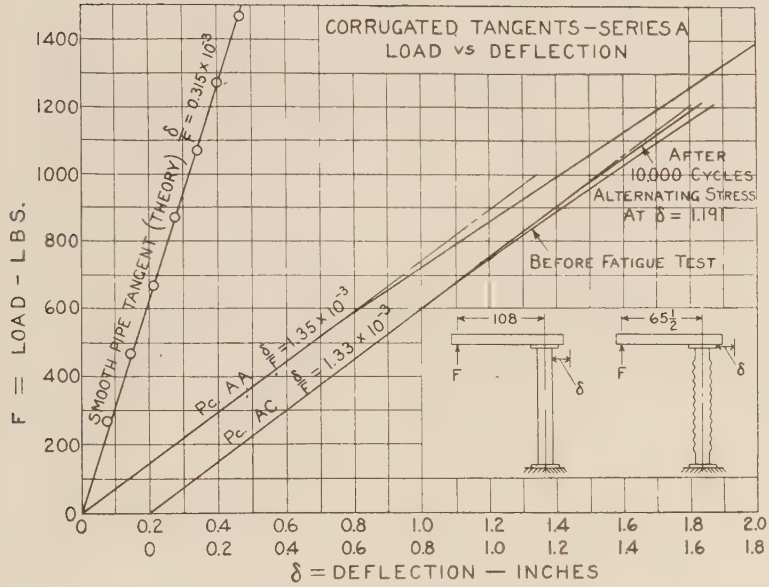
CORRUGATED TANGENTS—SERIES A
LOAD vs DEFLECTION
F = LOAD - LBS.
δ = DEFLECTION — INCHES
SMOOTH PIPE TANGENT (THEORY) δ = 0.315 x 10⁻³
Pc AA δ = 1.35 x 10⁻³
Pc AC δ = 1.33 x 10⁻³
AFTER 10,000 CYCLES ALTERNATING STRESS AT δ = 1.191
BEFORE FATIGUE TEST
108
65½
F
δ

PLATE XIII.

FIG. 1—LOAD-DEFLECTION CURVES FOR CORRUGATED TANGENTS, SERIES A.

This figure shows the load-deflection relationship for pieces AA and AC. The diagram in the lower right corner indicates the method of loading and the location of the deflection measurements. On this figure there is also shown the results of load-deflection measurements on a smooth pipe of the same basic dimensions as the corrugated tangent. The line at the left of the figure represents the load-deflection relationship according to theory as a result of computations using the moment-area method. The circles along this line are experimentally determined points. This demonstrates the exceedingly close agreement between the theoretical and experimental results.

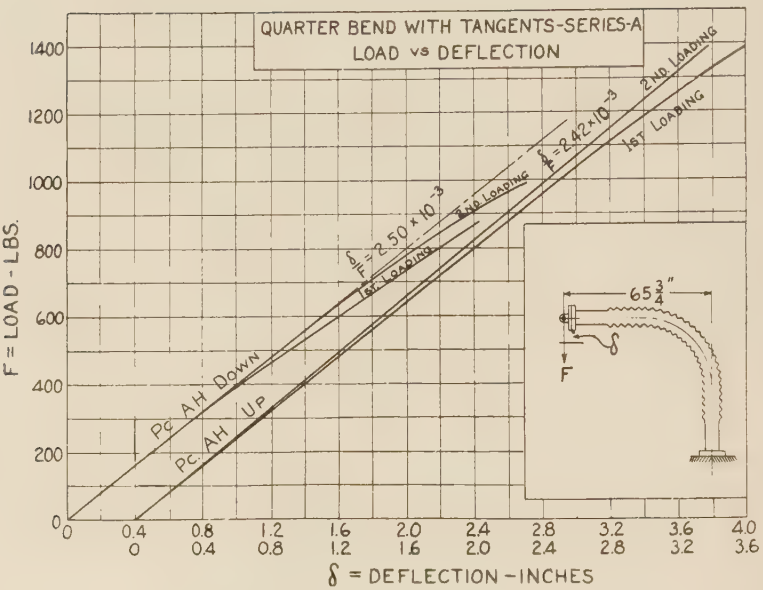

PLATE XIII.

FIG. 2—LOAD-DEFLECTION CURVES FOR CORRUGATED QUARTER-BENDS, SERIES A.

This figure shows the load-deflection relationship for piece AH. The diagram indicates the method of loading and the point of deflection measurements. The curves given represent the load-deflection for the pipe as received and again after a few stress cycles. It will be noted that the effect of the stress cycles is to raise the elastic limit of the pipe as a whole.

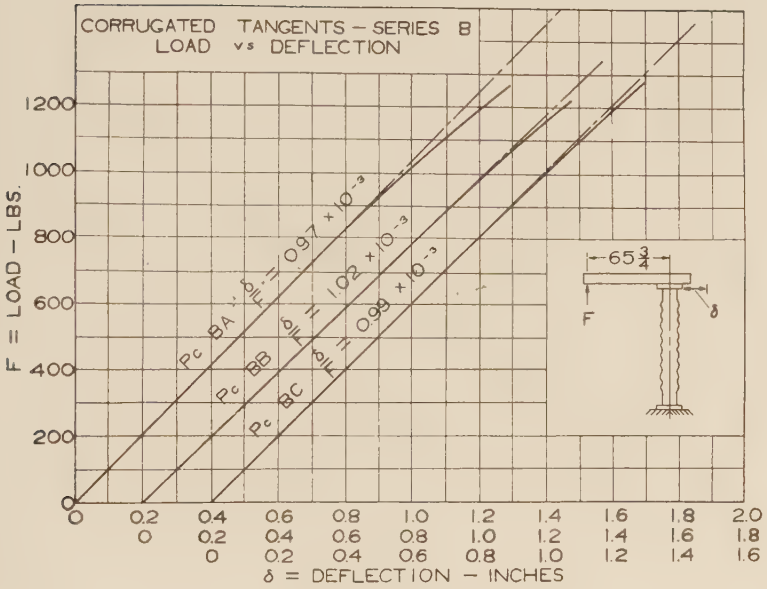

PLATE XIV.

FIG. 1—LOAD-DEFLECTION CURVES FOR CORRUGATED TANGENTS, SERIES B.

These curves show the load-deflection relationship for pieces B A, B B, and B C.

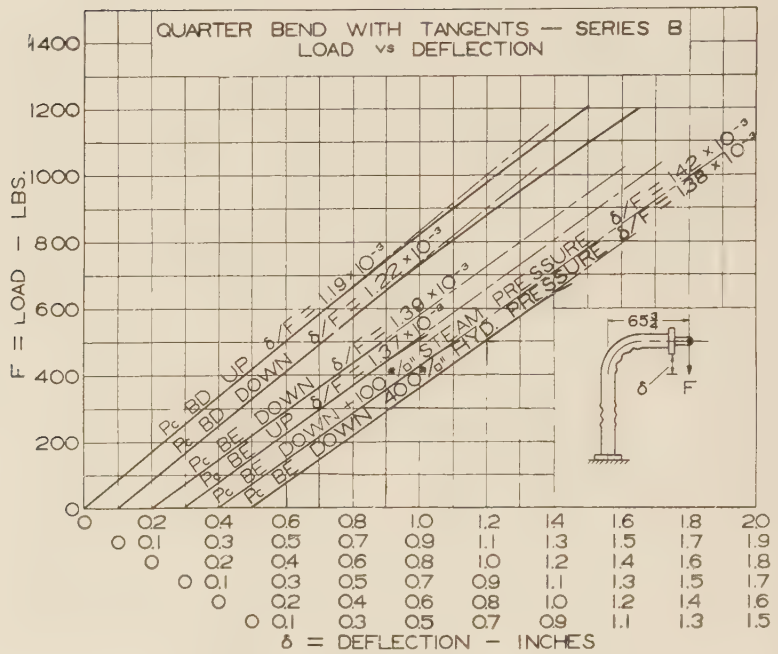
QUARTER BEND WITH TANGENTS — SERIES B
LOAD vs DEFLECTION
F = LOAD - LBS.
1400
1200
1000
800
600
400
200
0
δ = DEFLECTION - INCHES
Pc BD UP δ/F = 1.19 x 10⁻³
Pc BD DOWN δ/F = 1.22 x 10⁻³
Pc BE UP δ/F = 1.38 x 10⁻³
Pc BE DOWN δ/F = 1.37 x 10⁻³
Pc BE DOWN + 100 #/□" STEAM PRESSURE δ/F = 1.42 x 10⁻³
Pc BE DOWN 400 #/□" HYD PRESSURE δ/F = 1.38 x 10⁻³
65 3/4
δ
F

PLATE XIV.

FIG. 2—LOAD-DEFLECTION CURVES FOR QUARTER-BENDS WITH CREASED ARC AND CORRUGATED TANGENT, SERIES B.

These curves show the load-deflection relationship for pieces B D and B E. Note that the load-deflection curve for piece B F, under 400 pounds per square inch internal hydrostatic pressure is essentially the same as without internal pressure. The terms up and down applied to the curves, indicate the direction of the applied load at the free flange.

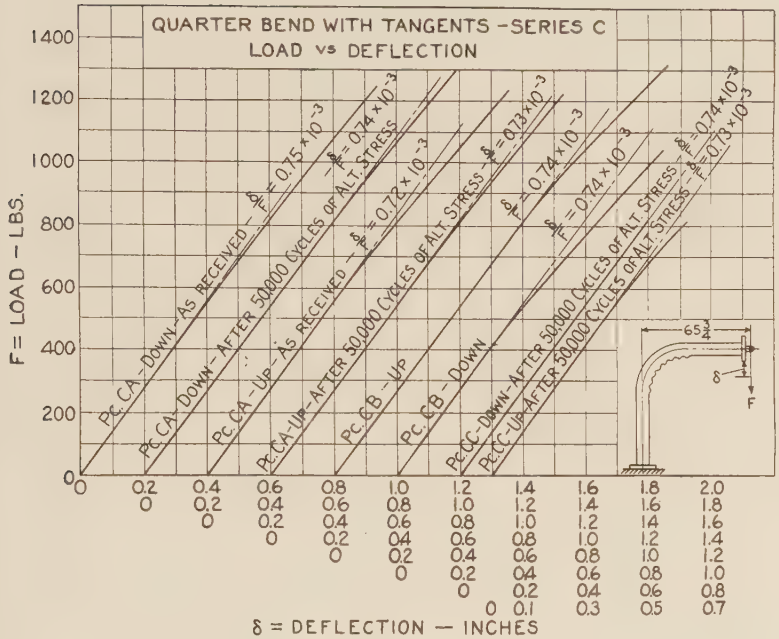
QUARTER BEND WITH TANGENTS -SERIES C
LOAD vs DEFLECTION
F = LOAD - LBS.
δ = DEFLECTION — INCHES
Pc. CA - DOWN - AS RECEIVED
Pc. CA - DOWN - AFTER 50000 CYCLES OF ALT. STRESS
Pc. CA - UP - AS RECEIVED
Pc. CA - UP - AFTER 50,000 CYCLES OF ALT. STRESS
Pc. CB - UP
Pc. CB - DOWN
Pc. CC - DOWN - AFTER 50000 CYCLES OF ALT. STRESS
Pc. CC - UP - AFTER 50000 CYCLES OF ALT. STRESS
65 3/4
δ
F

PLATE XV—LOAD-DEFLECTION CURVES FOR QUARTER-BENDS WITH CREASED ARC, SERIES C.

These curves show the load-deflection relationships for pieces C A, C B and C C. The effect of cold work on the raising of the primitive yield point is shown by the raising of the proportional limit of these curves after the pieces had been subjected to cycles of alternating stress.

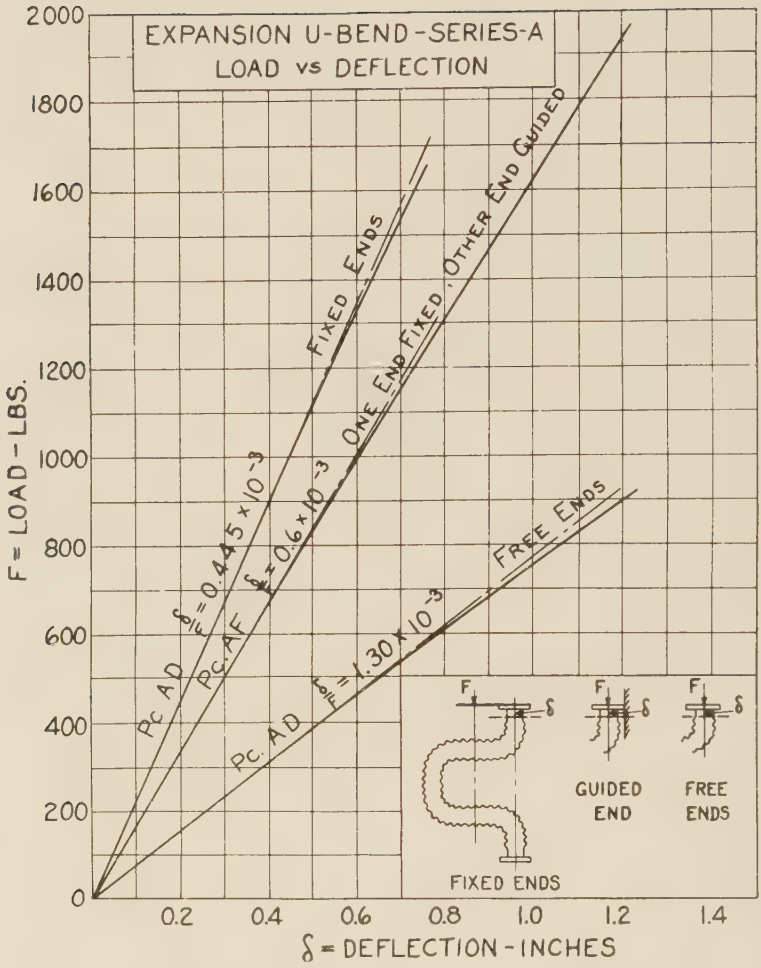

Plate XVI—Load-Deflection Curves for Expansion U-Bends, Series A.

These curves show the load-deflection relationship for pieces A D and A F. Three loading conditions are represented; fixed ends, one end fixed and the other end guided, and free ends. The free end and fixed end conditions are shown in Plates IX and X. For the guided end condition the U-bend was erected with the bend lying in a vertical plane in the pump type specific strain machine (Plate VII). The loading was applied, and measured, through a calibrated ring. In this test one end of the bend was fixed. The other end was attached to the pump rod through a horizontal pivot joint. The moving flange was thus allowed to rotate and its center was constrained by the pump rod to move in a horizontal line.

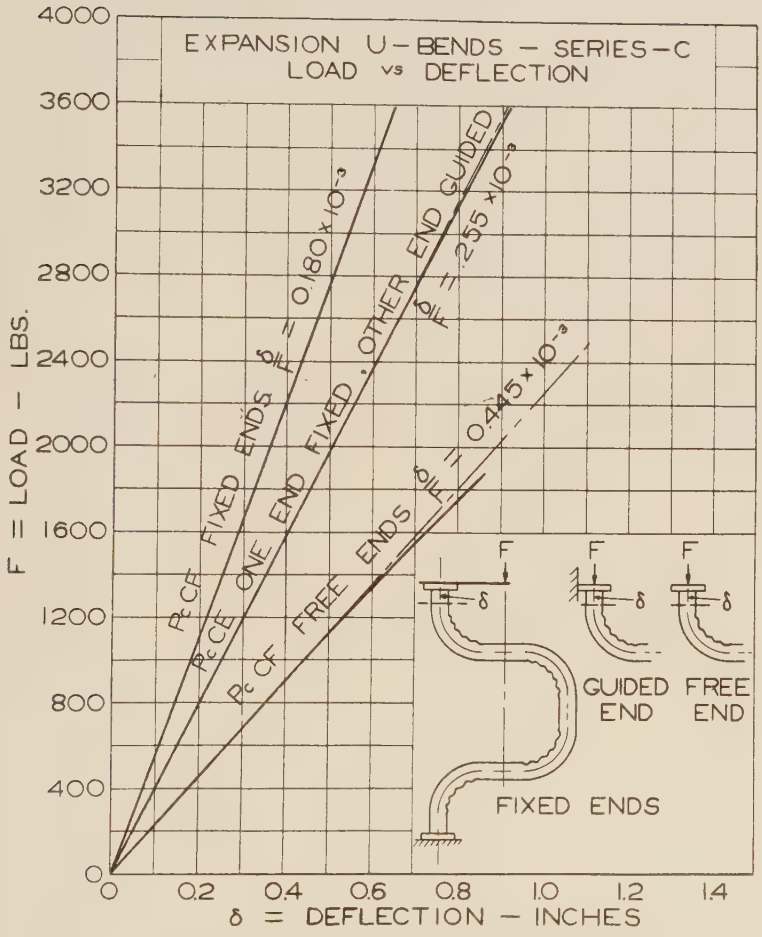

PLATE XVII—LOAD-DEFLECTION CURVES FOR EXPANSION U-BENDS, SERIES C.

These curves show the load-deflection relationships for Pieces C E and C F. The significance of the various loading conditions is explained in section 25.

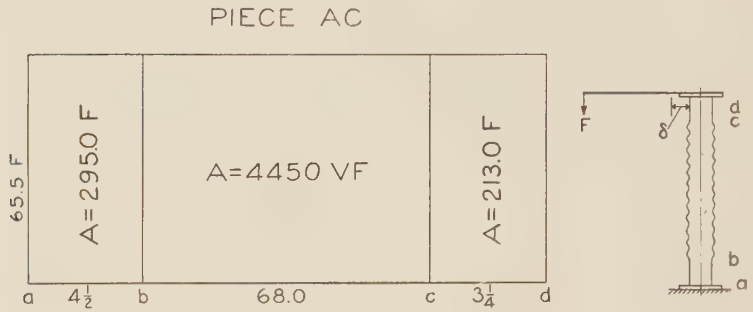

MOMENT AREA DIAGRAM

FIG. 1

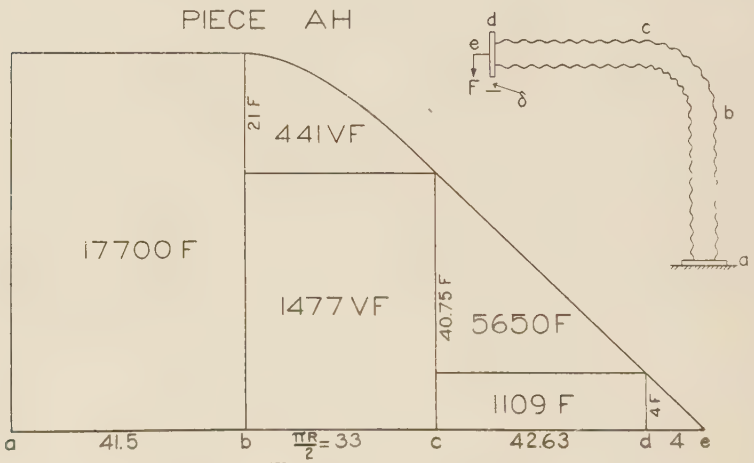

MOMENT AREA DIAGRAM

FIG. 2

PLATE XVIII—MOMENT-AREA DIAGRAMS FOR FLEXIBILITY COMPUTATIONS.

FIG. 1—MOMENT-AREA DIAGRAM FOR PIECE A C. THE COMPUTATION OF THE FLEXIBILITY FACTOR IS GIVEN IN SECTION 27.

FIG. 2—MOMENT-AREA DIAGRAM FOR PIECE A H. THE COMPUTATION OF THE FLEXIBILITY FACTOR IS GIVEN IN SECTION 28.

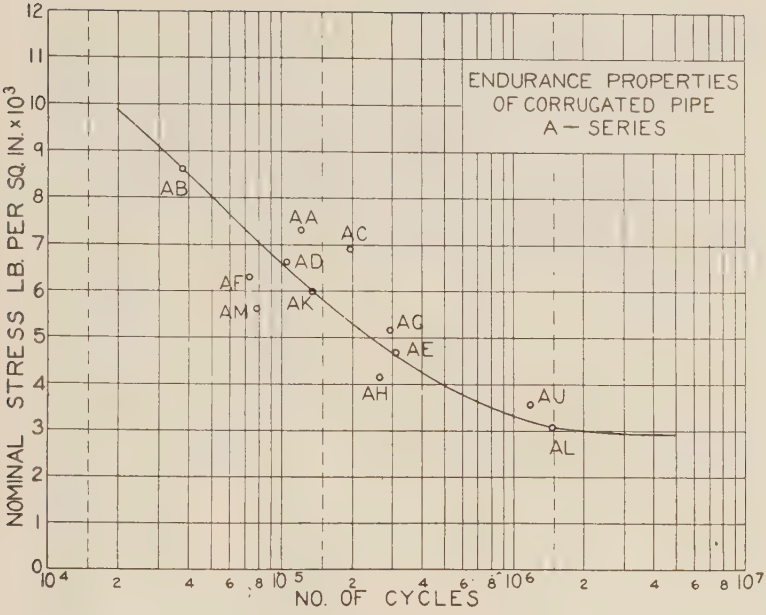

PLATE XIX—ENDURANCE PROPERTIES OF CORRUGATED PIPE, SERIES A.

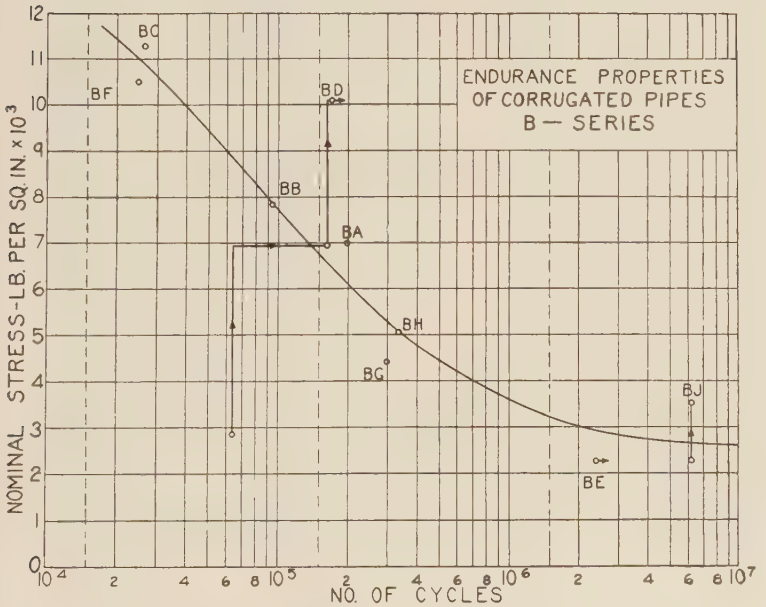

PLATE XX—ENDURANCE PROPERTIES OF CORRUGATED PIPE, SERIES B.

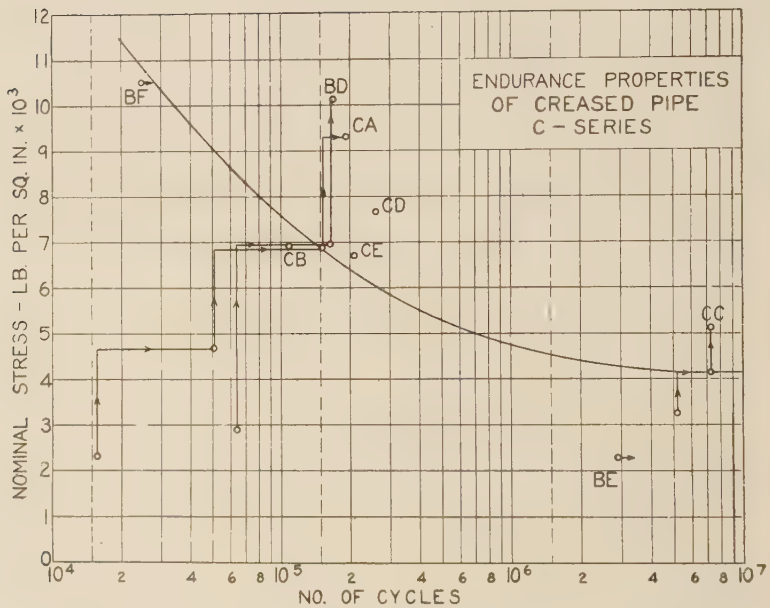

PLATE XXI—ENDURANCE PROPERTIES FOR CREASED PIPE, SERIES C.

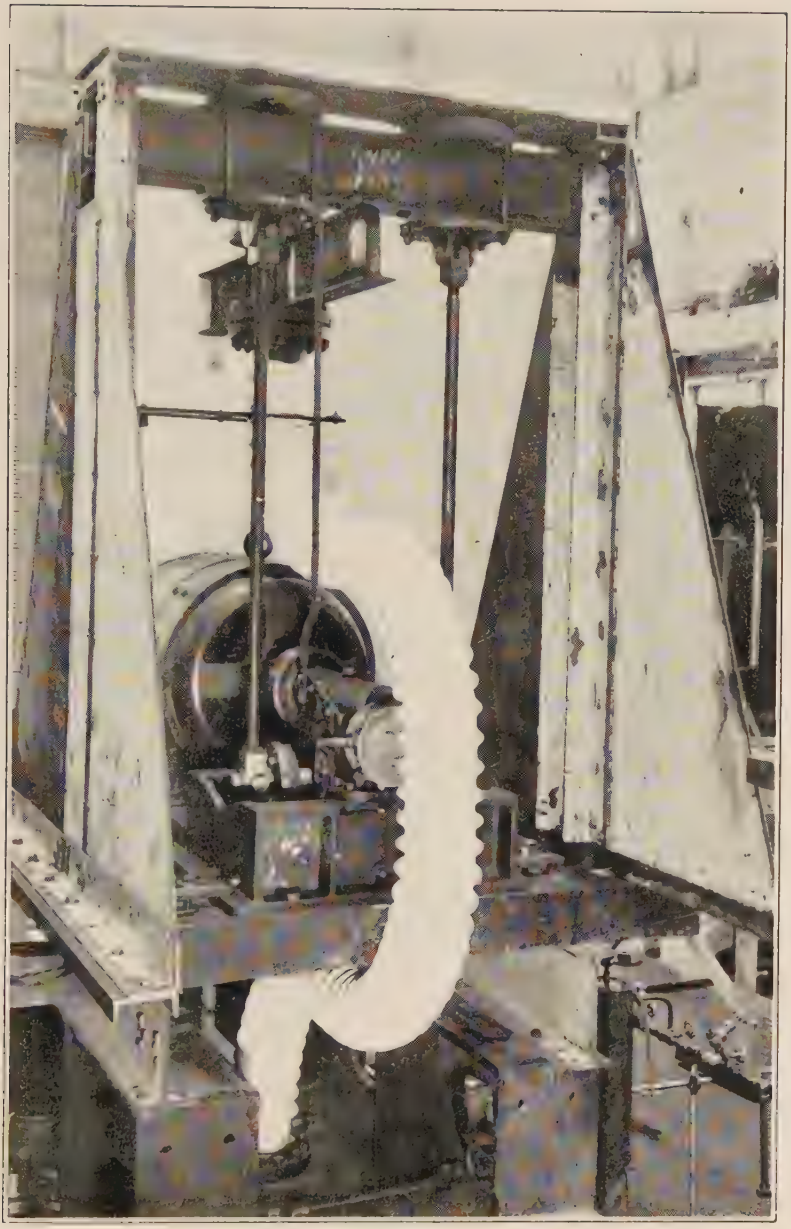

PLATE XXII—A CORRUGATED EXPANSION U-BEND ERECTED FOR FIXED-END TEST IN A SPECIFIC STRAIN TYPE FATIGUE TESTING MACHINE.

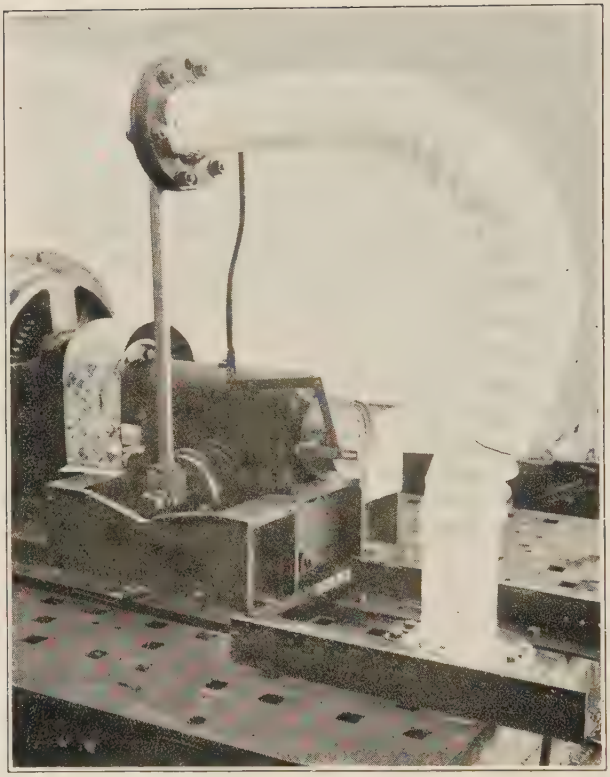

PLATE XXIII—THE SINGLE OFFSET QUARTER BEND AS ERECTED FOR TEST IN A SPECIFIC STRAIN TYPE FATIGUE TESTING MACHINE.

Note the crack, as a result of the fatigue test, which appears in the fourth corrugation from the bottom of the pipe.

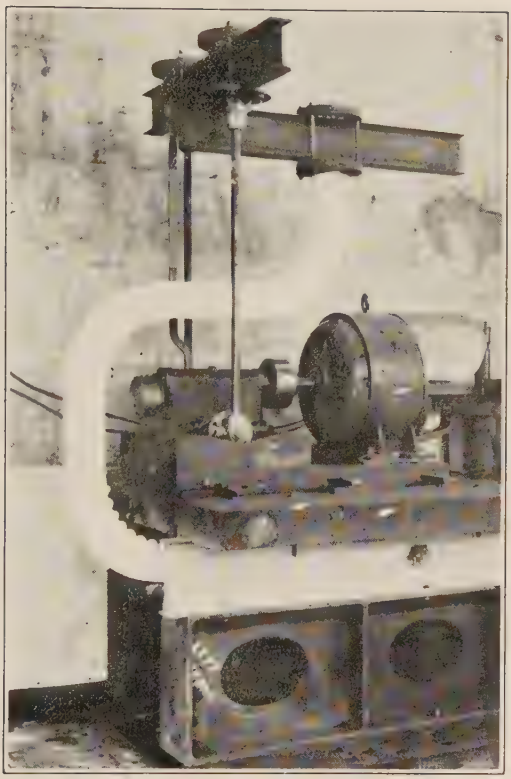

Plate XXIV—A Creased Expansion U-Bend Erected for Test in a Specific Strain Type Fatigue Testing Machine.

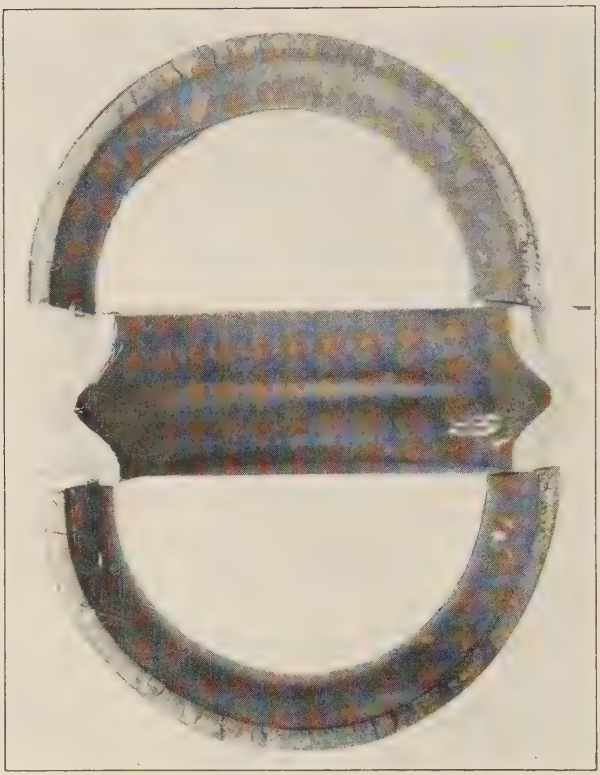

PLATE XXV—A FATIGUE FAILURE IN CORRUGATED PIPE, SERIES B.

This failure occurred in the rotating beam testing machine. The crack developed through the corrugation for about half the circumference. The pipe was sectioned by cutting out the failed corrugation and then by cutting through this corrugation along a pipe diameter. The two failed sections were laid back for the purpose of photographing. The appearance of the fracture indicates that the crack originated from the inner pipe surface.

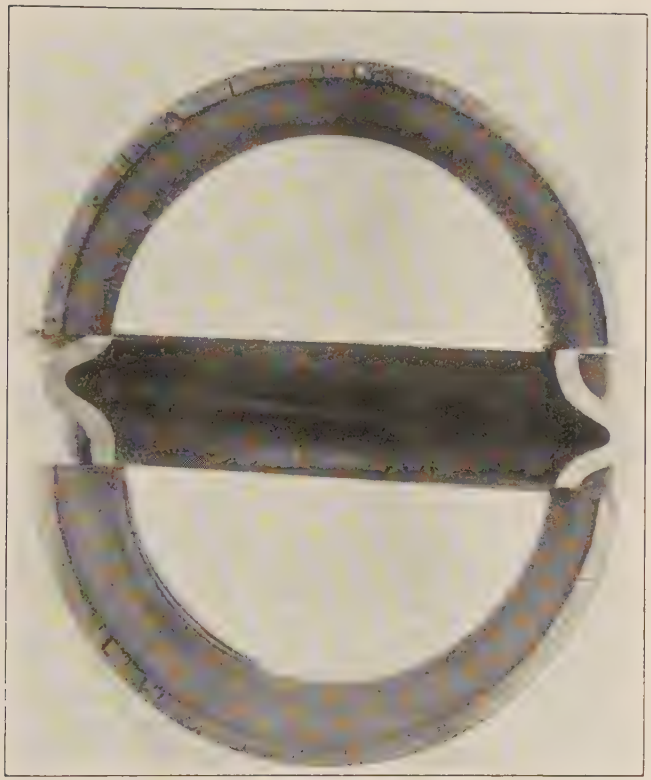

PLATE XXVI—A FATIGUE FAILURE IN CORRUGATED PIPE, SERIES A.

This failure occurred in a specific strain testing machine. The nature of the failure is similar to that occurring in the rotating beam machine as shown in Plate XXV. Here also the crack has progressed from the inner pipe wall to the outer surface.

PLATE XXVII—PHOTOMICROGRAPH OF FATIGUE FAILURE.
(Magnification x100.)

This specimen was removed from piece A M, the single offset quarter bend, in the plane of the bend at the crest of the corrugation next above the fracture. The inner pipe surface is at the top of the photograph. The crack had not developed sufficiently to work entirely through the pipe wall.

PLATE XXVIII—A FATIGUE FRACTURE IN A CREASED PIPE.

This view is of a trough between two creases and shows the location and appearance of a typical failure in the creased pipe.

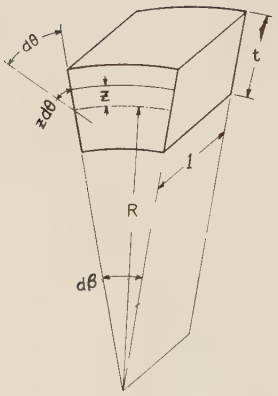

FIG 1

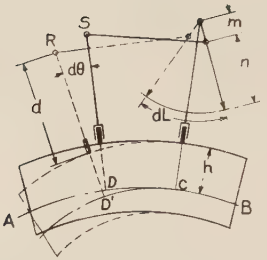

FIG. 2

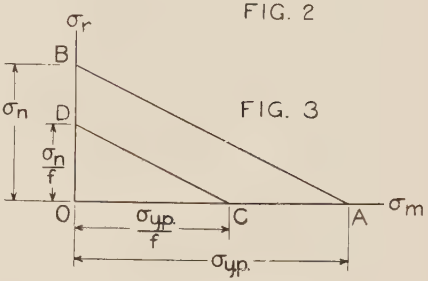

FIG. 3

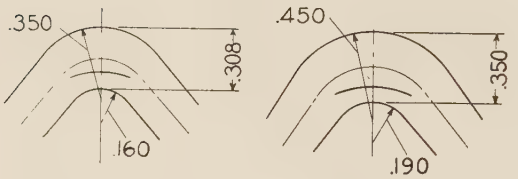

SERIES-A SERIES-B

FIG. 4

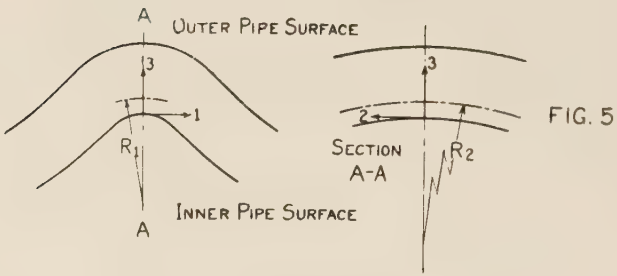

FIG. 5

PLATE XXIX.

FIG. 1—AN ELEMENT FROM A CURVED PLATE IN BENDING.

FIG. 2—A SCHEMATIC DIAGRAM OF THE ACTION OF THE BENDING STRAIN GAGE.

FIG. 3—TO ACCOMPANY SECTION 51, "THE METHOD OF DETERMINING SAFE WORKING STRESSES."

FIG. 4—THE SYSTEM OF AXES AND THE LOCATION OF R_1 AND R_2 FOR A CORRUGATED SECTION.

FIG. 5—TYPICAL CORRUGATION DIMENSIONS OBTAINED FROM AVERAGING MEASUREMENTS.

PLATE XXX—A VIEW OF THE HUGGENBERGER TENSOMETER.

PLATE XXXI—THE BENDING STRAIN GAGE.

This view shows the gage applied to measure the longitudinal strain at the crest of a corrugation. The small rods for the base of the gage may be seen on the corrugation at several stations for measurement. The rods in the circumferential, or hoop, direction are set at a 1-inch gage length, while the ones in the longitudinal direction are set at ¼-inch. A calibration of this instrument showed it to have a magnification factor of 40 when applied to measure longitudinal strains and a factor of 45 when applied to measure hoop strains.

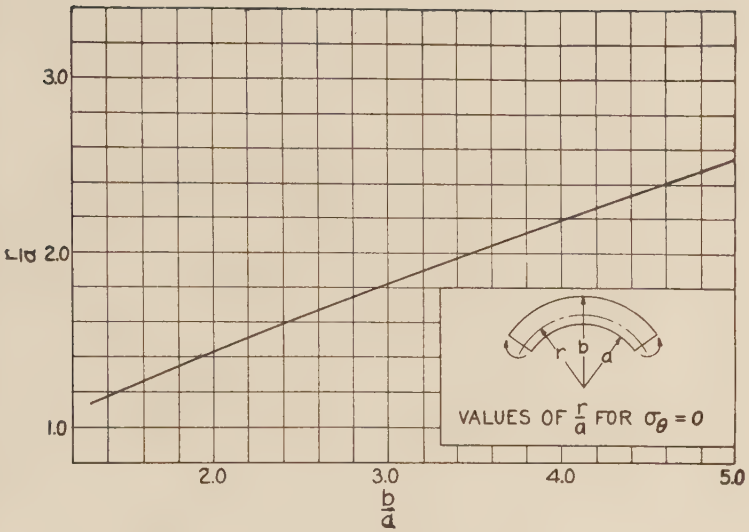

PLATE XXXII—POSITION OF NEUTRAL AXIS IN CURVED BARS.

The value of the ratio of the radii of curvatures of the neutral axis to the inner surface of a curved bar as a function of the value of the ratio of the radii of curvatures of the outer surface to the inner surface.

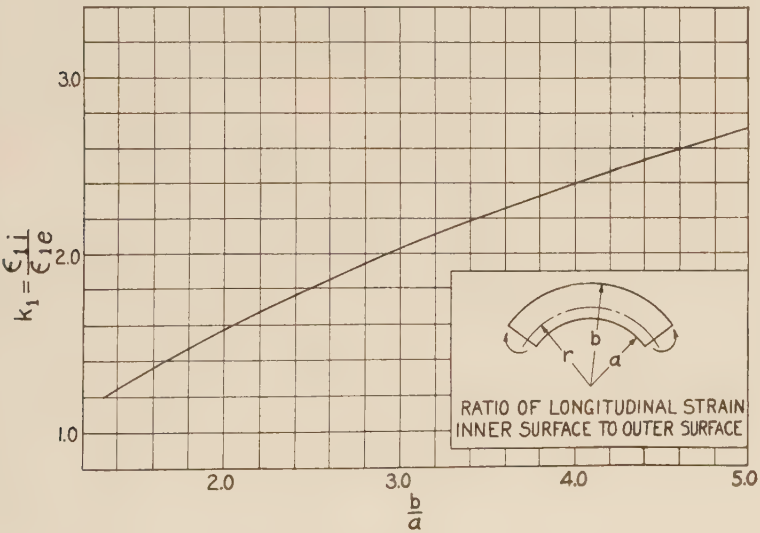

PLATE XXXIII—RATIO OF STRAINS, OUTER SURFACE TO INNER SURFACE IN CURVED BARS.

The absolute value of the ratio of the longitudinal strains at the outer surface to the inner surface of a curved bar in pure bending.

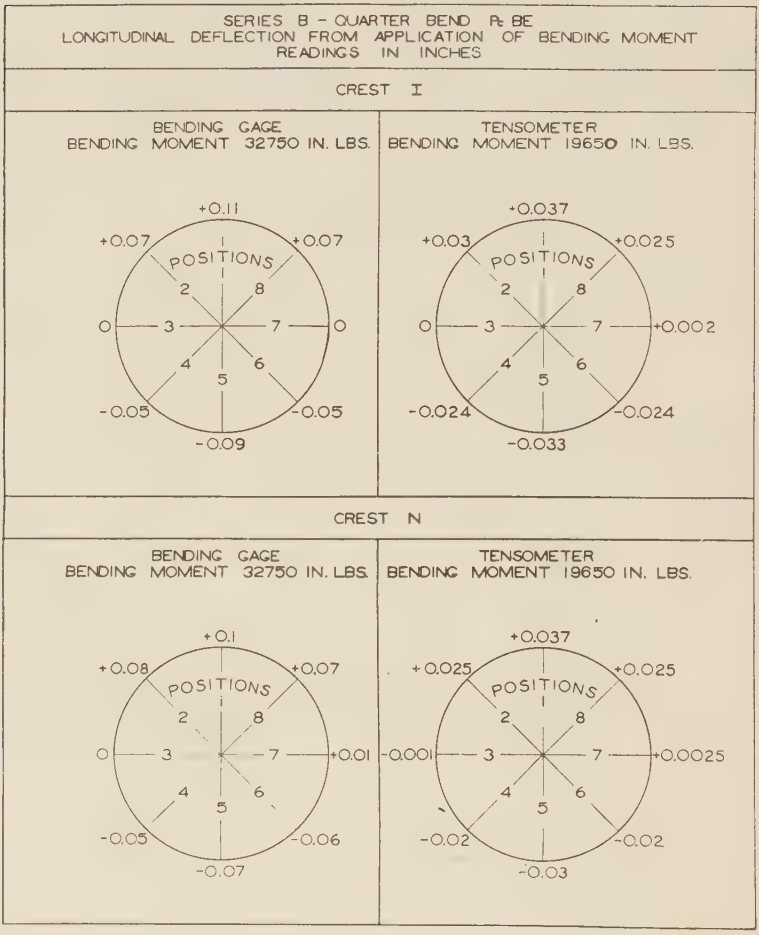

PLATE XXXIV—LONGITUDINAL STRAIN READINGS ON A CORRUGATION CREST, DUE TO BENDING MOMENT.

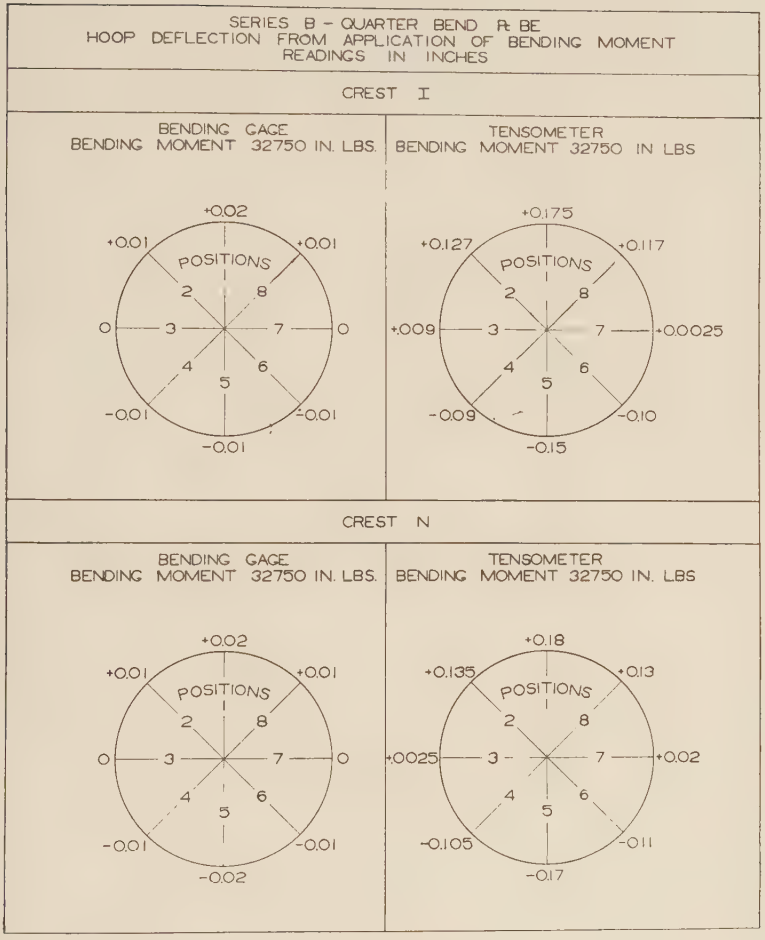

PLATE XXXV—HOOP STRAIN READINGS ON A CORRUGATED PIPE, DUE TO BENDING MOMENT.

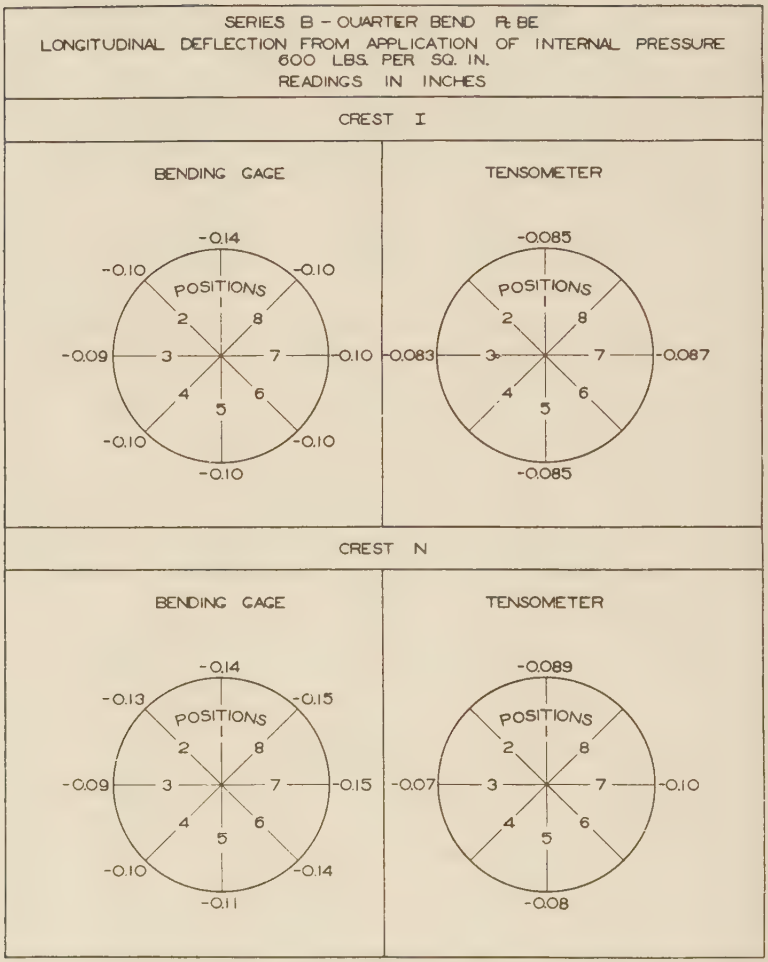

PLATE XXXVI—LONGITUDINAL STRAIN READINGS ON A CORRUGATED PIPE, DUE TO INTERNAL PRESSURE.

SERIES B – QUARTER BEND Pc BE
HOOP DEFLECTION FROM APPLICATION OF INTERNAL PRESSURE
600 LBS. PER SQ. IN.
READINGS IN INCHES

CREST I

BENDING GAGE	TENSOMETER
ALL READINGS = ZERO	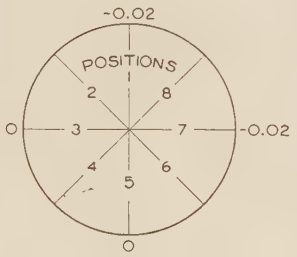

CREST N

BENDING GAGE	TENSOMETER
ALL READINGS = ZERO	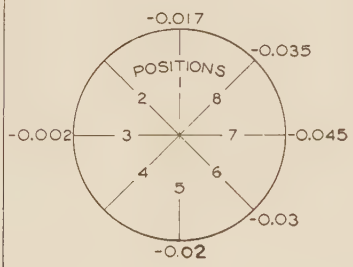

PLATE XXXVII—HOOP STRAIN READINGS ON A CORRUGATED PIPE, DUE TO INTERNAL PRESSURE.

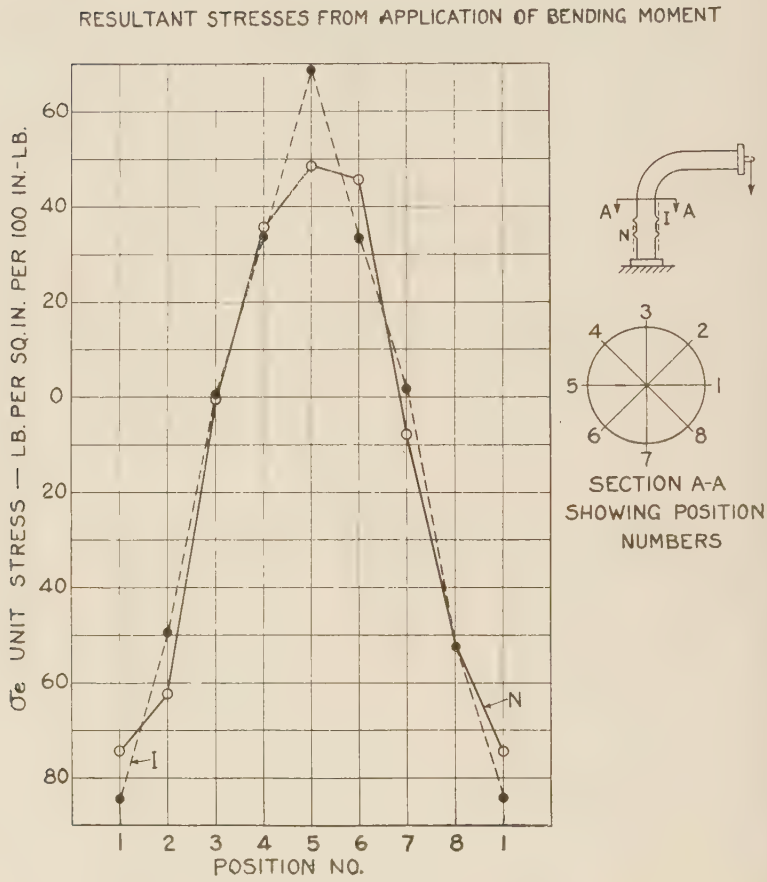

PLATE XXXVIII—THE VALUE OF EQUIVALENT STRESS AT THE CRESTS OF TWO CORRUGATIONS AT THE INNER PIPE SURFACE.

FROM "PIPING HANDBOOK" BY J H WALKER AND SABIN CROCKER SECOND EDITION		ψ ROTATION	δ_z	δ_x
CASE I FIXED END OF A CANTILEVER ROTATATED THRU AN ANGLE ψ			ψL	
CASE II STRAIGHT CANTILEVER ACTED ON BY A TRANSVERSE FORCE F AT THE FREE END	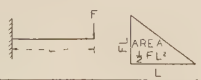	$\frac{1}{2}\frac{FL^2}{EI}$	$\psi\frac{2}{3}L$	
CASE III STRAIGHT CANTILEVER ACTED ON BY A MOMENT M AT THE FREE END	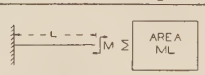	$\frac{ML}{EI}$	$\psi\frac{1}{2}L$	
CASE IV STRAIGHT CANTILEVER ACTED ON BY A TORSIONAL MOMENT M	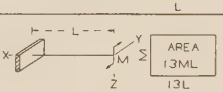	$\frac{1.3ML}{EI}$		
CASE V QUARTER BEND FIXED AT ONE END AND ACTED ON BY A RADIAL FORCE F IN PLANE OF BEND	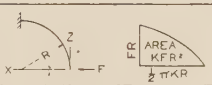	$\frac{KFR^2}{EI}$	ψ0.5 R	ψ0.7854 R
CASE VI QUARTER BEND FIXED AT ONE END AND ACTED ON BY AN AXIAL FORCE F IN PLANE OF BEND	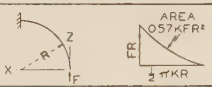	$\frac{0.57\,KFR^2}{EI}$	ψ0.624R	ψ0.876 R
CASE VII QUARTER BEND FIXED AT ONE END AND ACTED ON BY A BENDING MOMENT M IN PLANE OF BEND	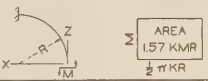	$\frac{1.5708\,KMR}{EI}$	ψ0.363 R	ψ0.637 R

		ψ_{zv}	ψ_{zv}	δ_{xv}	δ_{zv}	δ_v
CASE VIII QUARTER BEND FIXED AT ONE END AND ACTED ON BY A FORCE F ⊥ TO PLANE OF BEND	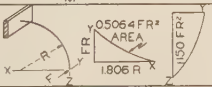	$\frac{.05064FR^2}{EI}$	$\frac{1.50FR^2}{EI}$	.0754Rψ$_{xv}$	.0754Rψ$_{xz}$	$\frac{.2485FR^3}{EI}$
CASE IX QUARTER BEND FIXED AT ONE END AND ACTED ON BY A MOMENT M IN A PLANE ⊥ TO PLANE OF BEND	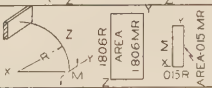	$\frac{0.5MR}{EI}$	$\frac{1.806MR}{EI}$	.0695Rψ$_{xv}$	.0695Rψ$_{xz}$	$\frac{1.150\,MR^2}{EI}$
CASE X QUARTER BEND FIXED AT ONE END AND ACTED ON BY A TORQUE MOMENT M IN A PLANE ⊥ TO FREE END OF BEND		$\frac{.806MR}{EI}$	$\frac{0.5MR}{EI}$	.0306Rψ$_{xv}$	.0306Rψ$_{xz}$	$\frac{.05064MR^2}{EI}$

PLATE XXXIX—THE ROTATIONS AND DEFLECTIONS OF A CANTILEVER AND A QUARTER BEND FOR VARIOUS LOADINGS.

These cases were taken from the "Piping Handbook" by Walker and Crocker.

COORDINATE AXES SELECTED SO THAT Z AXIS IS NORMAL TO THE ARC TANGENT AT THE FIXED END		
CASE XI FORCE AT FREE END ⊥ TO Z AXIS	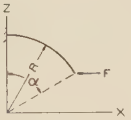	MOMENT = $FR(1-\cos\alpha)$ $\Psi F = \frac{KFR^2(\sin\alpha-\alpha\cos\alpha)}{EI}$ $\delta_x = \frac{KFR^3[\alpha(0.5+\cos^2\alpha)-1.5\sin\alpha\cos\alpha]}{EI}$ $\delta_z = \frac{KFR^3(0.5\sin^2\alpha-\alpha\sin\alpha\cos\alpha+\cos\alpha-\cos^2\alpha)}{EI}$
CASE XII FORCE AT FREE END ∥ TO Z AXIS	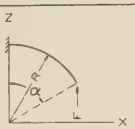	MOMENT = $FR\sin\alpha$ $\Psi F = \frac{KFR^2(\alpha\sin\alpha+\cos\alpha-1)}{EI}$ $\delta_x = \frac{KFR^3(1.5\sin^2\alpha-\alpha\sin\alpha\cos\alpha+\cos\alpha-1)}{EI}$ $\delta_z = \frac{KFR^3[\alpha(0.5+\sin^2\alpha)+1.5\sin\alpha\cos\alpha-2\sin\alpha]}{EI}$
CASE XIII MOMENT AT FREE END	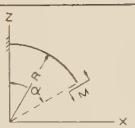	MOMENT = CONSTANT $\Psi M = \frac{KMR\alpha}{EI}$ $\delta_x = \frac{KMR^2(\sin\alpha-\alpha\cos\alpha)}{EI}$ $\delta_z = \frac{KMR^2(\alpha\sin\alpha+\cos\alpha-1)}{EI}$
COORDINATE AXES SELECTED SO THAT X AXIS IS NORMAL TO THE ARC TANGENT AT THE FREE END		
CASE XIV FORCE AT FREE END ⊥ TO X AXIS		MOMENT = $FR(1-\cos\alpha)$ $\Psi F = \frac{KFR^2(\alpha-\sin\alpha)}{EI}$ $\delta_x = \frac{KFR^3(1-\cos\alpha-0.5\sin^2\alpha)}{EI}$ $\delta_z = \frac{KFR^3(1.5\alpha-2\sin\alpha+0.5\sin\alpha\cos\alpha)}{EI}$
CASE XV FORCE AT FREE END ∥ TO X AXIS	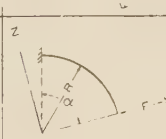	MOMENT = $FR\sin\alpha$ $\Psi F = \frac{KFR^2(1-\cos\alpha)}{EI}$ $\delta_x = \frac{KFR^3(0.5\alpha-0.5\sin\alpha\cos\alpha)}{EI}$ $\delta_z = \frac{KFR^3(1-\cos\alpha-0.5\sin^2\alpha)}{EI}$
CASE XVI MOMENT AT FREE END	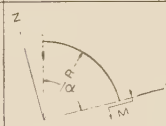	MOMENT = CONSTANT $\Psi M = \frac{KMR\alpha}{EI}$ $\delta_x = \frac{KMR^2(1-\cos\alpha)}{EI}$ $\delta_z = \frac{KMR^2(\alpha-\sin\alpha)}{EI}$

FROM A.S.M.E. TRANSACTIONS FSP-54-12

PLATE XI.—THE ROTATIONS AND DEFLECTIONS OF AN ARC OF LESS THAN 90 DEGREES UNDER VARIOUS LOADINGS.

These cases were taken from A.S.M.E. Transactions FSP-54-12 "Load Deflection Relations for Large Plain, Corrugated, and Creased Pipe Bends," by E. T. Cope and E. T. West.

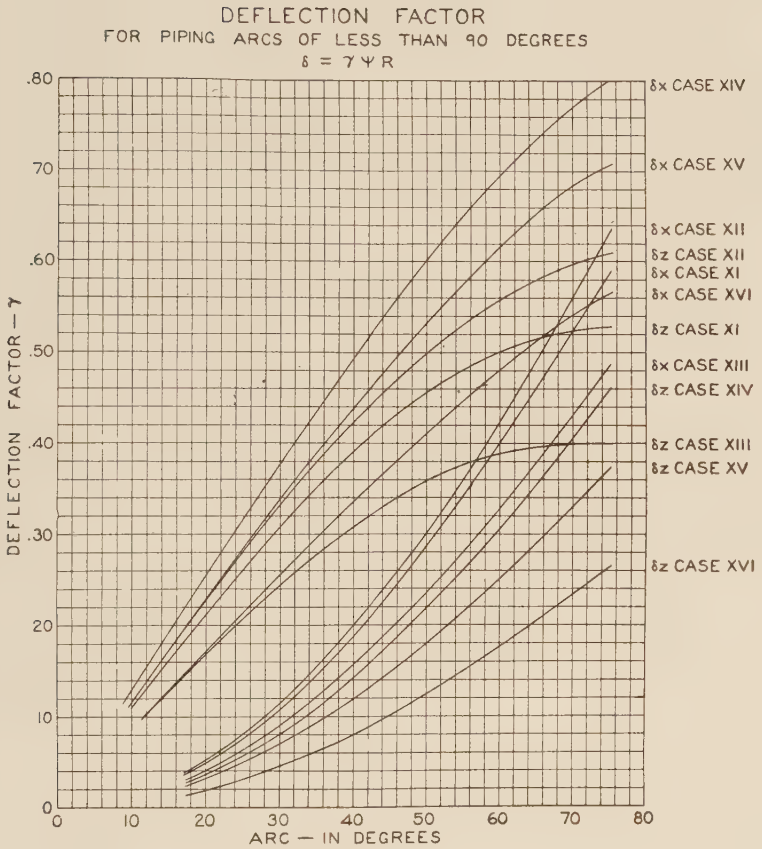

PLATE XLI—DEFLECTION FACTORS FOR AID IN COMPUTING DEFLECTIONS FOR ARCS LESS THAN 90 DEGREES.

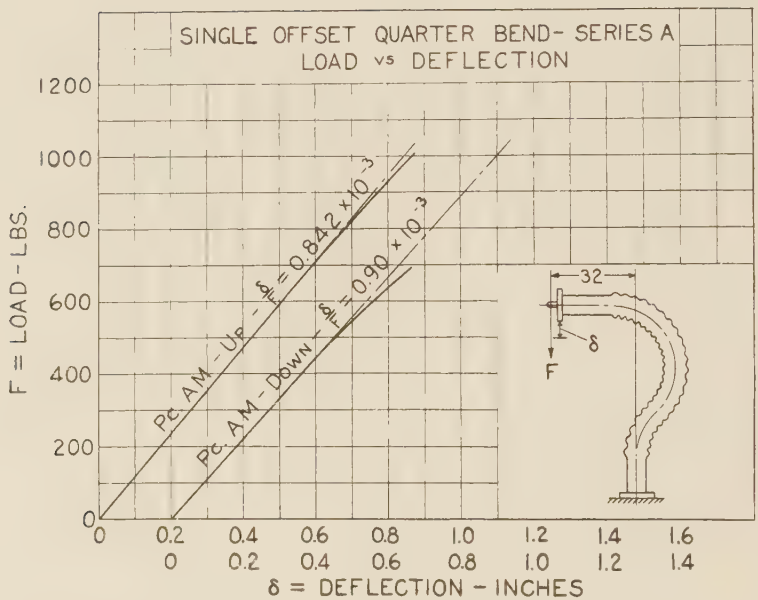

PLATE XLII—LOAD-DEFLECTION RELATIONSHIPS FOR THE SINGLE OFFSET QUARTER BEND, PIECE A M, SERIES A.

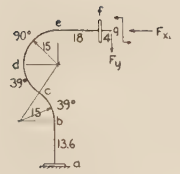

FIG 1

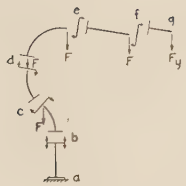

FIG. 2

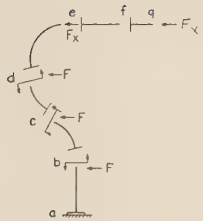

FIG 4

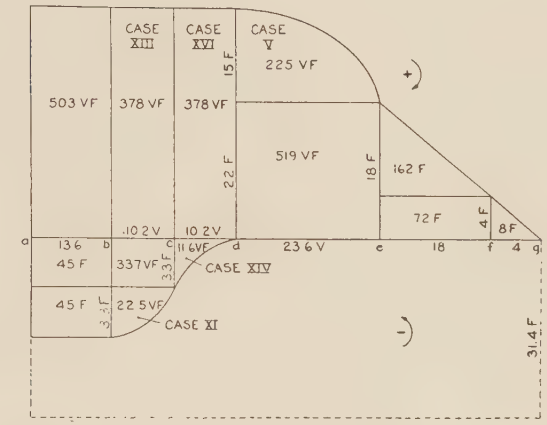

MOMENT AREA DIAGRAM FROM F_y AND RESTRAINING MOMENT

FIG. 3

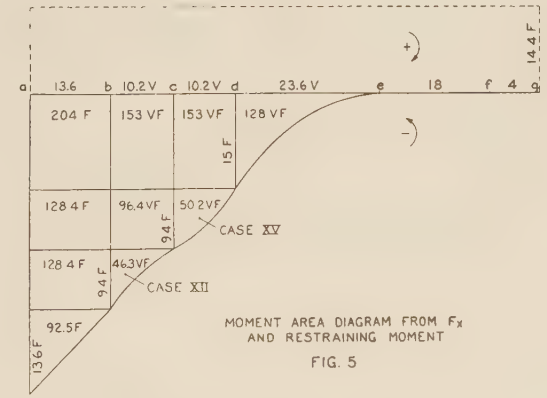

MOMENT AREA DIAGRAM FROM F_x AND RESTRAINING MOMENT

FIG. 5

PLATE XLIII—FIVE SKETCHES AND DIAGRAMS TO ACCOMPANY THE CALCULATIONS IN APPENDIX I.

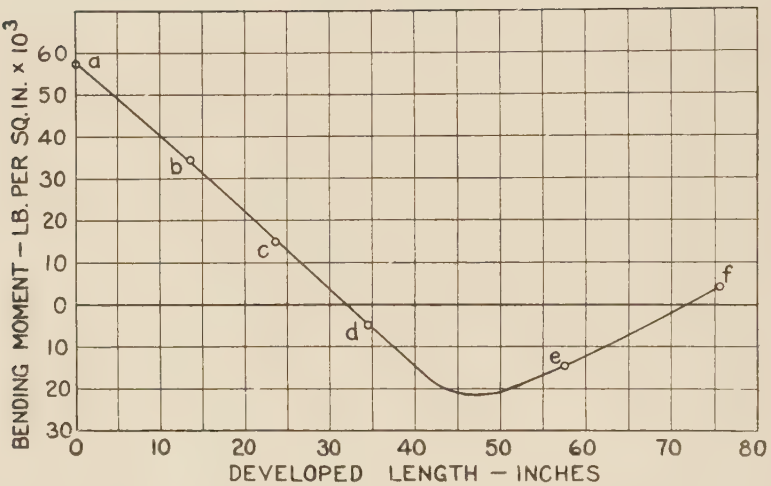

PLATE XLIV—A CURVE OF BENDING MOMENTS VERSUS DEVELOPED LENGTH FOR THE SINGLE OFFSET QUARTER BEND, AS DETERMINED IN APPENDIX I.

VITA.

Robert Lee Dennison, son of Ludovici Waters Dennison and Florence Lee Dennison, was born at Warren, Pennsylvania, on April 13th, 1901. He received his early education in the public schools of that city and in Kiskiminetas Spring School at Saltsburg, Pennsylvania. He entered the United States Naval Academy in 1919 and was graduated in 1923 with a commission as Ensign in the United States Navy. He served thereafter at sea in various types of combatant ships for a period of five years and later for three years. He attended the United States Naval Postgraduate School in 1928 and 1929, and the Pennsylvania State College in 1929 and 1930. He received the degree of Master of Science from this college in 1930. He now holds the rank of Lieutenant, and since July, 1933, has been the Superintendent of the Mechanical Engineering Laboratory at the United States Naval Engineering Experiment Station. He has for the past two years continued the study of engineering at the Johns Hopkins University.